Privacy-Preserving Mechanism for Collaborative Operation of High-Renewable Power Systems and Industrial Energy Hubs

Zare Oskouei, Morteza ; Mohammadi-ivatloo, Behnam; Abapour, Mehdi; Shafiee, Mahmood; Anvari-Moghaddam, Amjad

Published in:
Applied Energy

DOI (link to publication from Publisher):
10.1016/j.apenergy.2020.116338

Publication date:
2021

Document Version
Accepted author manuscript, peer reviewed version

Privacy-preserving mechanism for collaborative operation of high-renewable power systems and industrial energy hubs

Morteza Zare Oskouei[a], Behnam Mohammadi-Ivatloo[a,*], Mehdi Abapour[a], Mahmood Shafiee[b], Amjad Anvari-Moghaddam[a,c]

[a]*Smart Energy Systems Laboratory, Faculty of Electrical and Computer Engineering, University of Tabriz, Tabriz, Iran*
[b]*Mechanical Engineering Group, School of Engineering, University of Kent, Canterbury CT2 7NT, UK*
[c]*Department of Energy Technology, Aalborg University, 9220 Aalborg East, Denmark*

Abstract

Nowadays, achieving operational solutions to boost the flexibility of bulk power systems has become one of the major challenges in both industry and academia. The outcomes of recent studies demonstrate that the deployment of large-scale energy hubs can help enhance the flexibility of power systems. However, centralized management of networked energy hubs may not be compatible with the power system operator when they are managed by private owners. Motivated by this observation, a privacy-preserving decision-making structure is proposed in this paper for the collaborative operation of private industrial energy hubs and renewable power system by considering the high penetration of renewable energy sources. The proposed structure is drawn up based on the decentralized two-stage robust-stochastic approach and solved using the Benders decomposition algorithm by relying on the private ownership of various entities. The main objectives of this study lie in 1) decreasing renewable power curtailment and 2) minimizing the total operation costs of the private entities. To achieve these objectives, the effects of the multi-energy demand response program and energy conversion facilities are investigated in the context of the developed model. The competency and robustness of the proposed collaborative decision-making structure are examined on the IEEE 30-bus test system using GAMS and DIgSILENT PowerFactory software. Results show that if industrial energy hubs are successfully deployed in industrial parks, the total operation cost of the renewable power system decreases by up to 16.33%, renewable power curtailment reduces by 92.9%, and flexibility of the renewable power system enhances by increasing spinning reserve.

Keywords: Benders decomposition, demand response programs, energy storage systems, energy hub systems, privacy-preserving collaboration, renewable power curtailment.

Nomenclature

Indices (sets)

d ($\mathcal{D}$)	Index of blocks of the piecewise linearization of the quadratic cost function.
g, e ($\mathcal{G}$, $\mathcal{E}$)	Indices of thermal units and electrical energy storages.
h ($\mathcal{H}$)	Index of industrial energy hubs.
i, j ($\mathcal{I}$)	Indices of transmission buses.
k, q ($\mathcal{K}$, $\mathcal{Q}$)	Indices of CHP units and P2H storages.

*Corresponding author
Email address: bmohammadi@tabrizu.ac.ir (Behnam Mohammadi-Ivatloo)

l, n ($\mathcal{L}$, $\mathcal{N}$)	Indices of electrical and heat loads connected to industrial energy hubs.
m ($\mathcal{M}$)	Index of electrical loads connected to renewable power system.
s ($\mathcal{S}$)	Index of scenarios.
t ($\mathcal{T}$)	Index of hourly intervals.
$w(\mathcal{W})$, p ($\mathcal{P}$)	Indices of WFs and PV parks.
Parameters	
a_g, b_g, c_g	Fuel consumption cost coefficients of thermal unit g.
COP_q	Coefficient of P2H storage performance.
$C^d_{g,in}$, $C^d_{g,fi}$	Initial and final amounts of generation cost in block d of the linearized cost function of thermal unit g.
IE, IH	Rate of incentive for electrical and heat demands variation.
$KN_{i,\Xi}$, $KN_{h,\Xi}$	Bus-Ξ and hub-Ξ incidence matrices.
$PD_{m,t}$	Forecasted electric demand at hour t.
$PD^{ini}_{l,t,s}$, $HD^{ini}_{n,t,s}$	Initial electrical and heat demands connected to industrial energy hubs.
RU_g, RD_g	Ramping up/down limits of thermal unit g.
t_b	Iteration numbers for Benders decomposition.
x_{ij}	Equivalent reactance of line ij.
XG^{on}_g, XG^{off}_g	Minimum on/off times of thermal unit g.
$P^f_{w,t}$, $P^f_{p,t}$	Forecasted renewable power output of WF w and PV park p at hour t.
$P^d_{g,in}$, $P^d_{g,fi}$	Initial and final amounts of power produced in block d of the linearized cost function of thermal unit g.
$\tilde{P}_{w,t}$, $\tilde{P}_{p,t}$	Maximum deviation of WF w and PV park p from forecasted values at hour t.
$\hat{P}_{t_b,h,t,s}$	The amount of exchanged power, which is determined in the master problem.
SU_g, SD_g	Start-up/shut-down ramp limit of thermal unit g.
UT^0_g, DT^0_g	Duration of periods that thermal unit g has been online/offline prior to the first interval of the operating horizon.
Z^d_g	The slope of each block of the linearized cost function of thermal unit g.
ΔP^d_g	Length of each block of the linearized cost function of thermal unit g.
λ_g, HV	Natural gas price and natural gas heat value.
ρ_k, ρ_e, ρ_q	Maintenance cost of CHP unit, electrical storage, and P2H storage.
$\eta_{(\cdot)}$	Efficiency coefficient of various units.
α_l, α_n	Participation rate of electrical and heat demands in multi-energy DRP.
Γ_t	Uncertainty budget of renewable generation.
Π_{re}	Penalty prices for wind and solar power curtailments.
σ_s	Probability of each scenario.
$\underline{(\cdot)}$, $\overline{(\cdot)}$	Minimum/maximum bounds of variables.
Variables	
$A_{(\cdot),t,s}$	Energy level of electrical and P2H storages at hour t in scenario s.
$C^{CHP}_{k,s}$, $C^{ES}_{e,s}$, $C^{P2H}_{q,s}$	The operation cost of CHP unit k, electrical storage e, and P2H storage q in scenario s.
$C^{MDR}_{l,n,s}$	Incentive compensation cost of multi-energy DRP in scenario s.
C^{RPS}, C^{IEH}_h	The total operation cost of renewable power system and industrial energy hub h.

$\hat{F}^{IEH}_{t_b,h,t,s}$	Minimized sum of slack variables for industrial energy hub h at iteration t_b.
$H_{(\cdot),t,s}$	Heating stored/supplied by IEHs' facilities at hour t in scenario s.
$H^{dir}_{q,t,s}$	Heat production by P2H storage q in direct mode of action at hour t in scenario s.
$\hat{O}^{IEH}_{t_b,h}$, $\hat{O}^{Total}_{t_b}$	The optimal operation cost of industrial energy hub h and total operational cost at iteration t_b.
$P_{(\cdot),t,s}$	Power drawn and released by various units at hour t in scenario s.
$p^{d}_{g,t,s}$	The power produced in block d of the piecewise linear cost function of thermal unit g at hour t in scenario s.
$P^{lo}_{g,t}$, $P^{up}_{g,t}$	Minimum/maximum available power output of thermal unit g at hour t.
$PC_{w,t,s}$, $PC_{p,t,s}$	Wind and solar power curtailments of WF w and PV park p at hour t in scenario s.
$PF_{ij,t,s}$	Power flow on line ij at hour t in scenario s.
$PD^{dr}_{l,t,s}$, $HD^{dr}_{n,t,s}$	Final electrical and heat demands profile at hour t in scenario s.
$SUC_{g,t}$, $SDC_{g,t}$	Start-up/shut-down costs of thermal unit g at hour t.
$\Delta P^{up}_{l,t,s}$, $\Delta P^{dw}_{l,t,s}$	Electrical demands change after multi-energy DRP implementation at hour t in scenario s.
$\Delta H^{up}_{n,t,s}$, $\Delta H^{dw}_{n,t,s}$	Heat demands change after multi-energy DRP implementation at hour t in scenario s.
$\delta_{i,t,s}$	Voltage phase angle at bus i at hour t in scenario s.
$u_{(\cdot),t,s}$	Binary variable to indicate status of facilities.
$y_{g,t}$, $\gamma_{g,t}$	Binary variable to indicate the status of thermal unit g at hour t.
$\tau^{P}_{t_b,h,t,s}$, $\Lambda^{P}_{t_b,h,t,s}$	Dual variables to create the optimality cutting plane and feasibility cutting plane.
$\xi^{P1}_{h,t,s}$, $\xi^{P2}_{h,t,s}$	Slack variables for the feasibility check.
$\beta_{w,t,s}$, $\beta_{p,t,s}$	Degree of the output power uncertainty of WF w and PV park p at hour t.
$r_{x,t,s}$, $\varepsilon_{t,s}$	Auxiliary variables in robust optimization model.
Functions	
$F_g(P_{g,t,s})$	Fuel cost function of thermal unit g at hour t in scenario s.

1. Introduction

1.1. Motivation and significance

Nowadays, due to lack of proper facilities, such as lines' capacity, as well as ever-escalating power consumption, restructured power systems face fundamental challenges to guarantee the stable operation of the entire power system and satisfy technical constraints [1]. At the generation side, the penetration of intermittent renewable energy sources (RESs) in power systems has dramatically increased, owing to concerns about rising energy prices [2], environmental problems [3], and reliability requirements [3]. Although the utilization of high-power RESs, such as wind farms (WFs) and photovoltaic (PV) parks has been proven to be an effective solution to address the existing concerns, the inherent variability and non-uniform distribution of these sources have posed remarkable challenges for the safe operation of renewable-based power systems [4]. According to some strong evidence, due to the aging of power systems infrastructure, renewable power system operators (RPSOs) are obligated to curtail a significant percentage of produced renewable power, especially at high penetration levels, to maintain the stability and reliability of power systems [5].

On the other hand, running on-site generation in large subscribers sites, e.g., industrial parks, has received considerable attention in recent years. For example, on-site energy production in the industrial sector of the U.S. in 2012 accounted for about 4% of the total power produced in the same year [6]. Accordingly, industrial parks have become one of the most influential players in the electrical industry with the significant development they have had in recent years. The strategic role of industrial parks in advancing power systems plans was extensively evaluated in recent studies from the perspective of industrial consumers [7] and RPSO [8]. Most of these studies have emphasized the use of backup power sources like electrical energy storage (EES) or energy conversion facilities to continuously supply industrial demands [9]. Therefore, it is obvious that the traditional power systems and the installed protection equipment are not suitable for compensating the excessive generation/load, yet upgrading the existing power systems for short periods of operation is not economical.

Thanks to the recent advances in the modernization of interconnected energy systems, energy hub systems have emerged as a promising platform in the form of multi-vector energy systems to overcome the technical challenges as well as mitigate the potential risks associated with various players in power systems [10]. The energy hub systems are composed of multiple input/output ports that create a stable interface between different energy networks with regards to the advanced energy conversion facilities and energy storage systems. These systems can provide unique economic and technical benefits for energy market players and energy network operators and planners [11]. From the power system operators' point of view, energy hub systems can boost the flexibility and reliability of power systems, enhance the resiliency of the system, reduce operation cost, and decrease energy-wasting [12]. In addition, from the perspective of energy system planners, the establishment of energy hubs in industrial parks, as a major energy consumer [13], can help to realize the theory of localization of sustainable energy production and consumption [14]. Implementing this mechanism not only increases the flexibility of the interconnected energy systems but also enables industrial consumers to actively participate in wholesale energy markets and take advantage of existing opportunities in different layers of energy networks [15]. On this basis, the industrial energy hubs (IEHs) could be networked to form a multi-vector community at the sub-transmission and transmission levels. In these circumstances, each IEH is managed by a private owner, which aims to supply local demands using the existing facilities in energy hubs or via bilateral energy exchange with wholesale energy markets at the lowest operating cost. The private IEHs are recognized as independent entities, and these entities should cooperate with the power system in a privacy-preserving way [16]. Moreover, the technical constraints must not be sacrificed to the existed distributed mechanisms. Accordingly, ensuring the optimal collaborative operation of multiple private IEHs and power systems without compromising privacy provisions is a challenging problem, especially when the various uncertainties are considered in the scheduling process [17]. Therefore, it is necessary to draw up a holistic decentralized decision-making structure for the coordinated operation of private IEHs and power systems to determine the optimal energy dispatch among various players in the wholesale energy markets. By doing so, the power system operator and industrial energy hub operators (IEHOs) can separately pursue their own goals within the framework of the restructured energy systems.

In the following, various studies on the optimal operation of networked energy hubs are briefly reviewed

and then the technical contributions of this paper are presented.

1.2. Related literature

Due to the scope of this paper, there exists a large body of related studies that were focused on optimal operation of networked energy hubs in power systems by incorporating RESs. In general, the related literature is categorized according to whether optimization programs were provided based on a traditionally centralized dispatch approach or a decentralized framework. In terms of the centralized energy dispatch of networked energy hubs, authors of [18] presented a centralized optimal energy management strategy for the coordinated operation of grid-connected energy hubs and the regional power system with the aim of decreasing wind power curtailment. In the same work, the decision-making about the integrated operation of the power system and energy hubs was made by a common master controller in a centralized manner. A robust operation strategy for networked energy hubs was presented in [19] considering the uncertainty of renewable power production and demand response programs (DRP). The main aim of that work was to reduce the total operation cost of multiple energy hubs during the scheduling interval. In [20], a cost-effective centralized program was developed for microgrids embedded with energy hubs with regards to the stochastic programming method and DRPs. In a different approach, a multi-objective optimization program was developed in [21] with the aims of minimizing the total operation cost of multiple energy hubs as well as reducing greenhouse gas emissions. In this work, the produced power by RESs was considered as an uncertain parameter and was modeled by a scenario-based method. A temporally-coordinated optimal operation strategy was developed in [22] for optimal energy management of a multi-energy system in both day-ahead and intra-day markets. A multi-step linearization method for the interconnected energy hubs was examined in [23], which minimized the total operational cost of the networked energy hubs during the scheduling period. In [24], an energy dispatch model was investigated for analyzing the performance of a multi-energy system in both the grid-connected and islanded modes. Moreover, in [25], a two-level optimization problem was proposed for determining optimal bidding/offering strategy of multiple networked energy hubs in the day-ahead electricity market considering different sources of uncertainty. The problem was developed in the form of the centralized dispatch approach, which was managed by the power system operator.

In addition to the utilized centralized decision-making schemes, there have been considerable efforts in the research community to integrate energy hubs into power systems in decentralized and privacy-preserving manners. In these kinds of studies, various distributed methods, such as the alternating direction method of multipliers (ADMM) and decomposition methods, were established to define decentralized optimization problems for sustainable exploitation of networked energy hubs. For example, in [26], a distributed energy management framework was derived from the ADMM method to determine the optimal scheduling of networked energy hubs. Authors of [27] proposed an auction-based regulation service mechanism for economic dispatch of the large-scale energy hubs in the context of the wholesale electricity market. The proposed mechanism was solved in a decentralized manner using the ADMM technique. In [28], a distributed robust optimization method was proposed for making private coordination between energy hubs and the power system considering the market price uncertainty. In that work, robust optimization

was considered to realize the worst-case of uncertain parameters in multi-carrier energy systems. In [29], the leader-follower theory was applied in the framework of Benders decomposition for the optimal dispatch of networked energy hubs. This theory can establish privacy-preserving collaborations among individual energy hub operators and the power system operator. Finally, in [30], distributed energy management methods based on the decomposition algorithm were proposed for the robust optimal energy dispatch of grid-connected energy hubs considering the uncertainty of renewable power generation. Likewise, authors of [31] developed a distributionally robust unit commitment algorithm for optimal energy management of the large-scale energy hubs with the aim of minimizing the total operation cost.

By examining the above-mentioned studies, it can be seen that the principal focus of the technical literature was on the optimal exploitation of multiple networked energy hubs aimed at reducing the total operation cost of the multi-carrier energy systems. Nevertheless, ignoring the challenges posed by the high penetration of RESs is the major gap in the aforementioned studies. It is worthwhile to mention that, to the best of our knowledge, no prior study in this field investigated the effects of new energy conversion facilities, such as power-to-heat (P2H) storage, on improving the performance of the integrated renewable energy systems in the presence of flexible demands and high-power and large-scale RESs. In addition, very few studies in the literature have addressed the unique benefits of multi-energy DRP in advancing the desired objectives of the energy system operators. Overall, we argue that the previous literature lacks detailed models to address the various flexibility options, so further studies are needed to design a holistic decision-making framework with respect to all available flexibility options.

1.3. Technical contributions and paper structure

This work aims to fill the knowledge gaps mentioned in the previous sub-section by applying a purely mathematical-technical perspective. To this end, a privacy-preserving structure is presented for optimizing RPSO/IEHOs collaborations in an iterative manner by considering high penetration of WFs and PV parks. The main objectives of the distributed optimization problem are to minimize the total operation cost of the renewable power system and IEHs, reduce renewable power curtailment, and enhance the flexibility of the integrated renewable energy system via realizing optimal coordination between different players. To clarify the main contributions of this paper, the features of the proposed model are compared with other published papers in Table 1. Eventually, the technical contributions of this study are as follow:

(1) A scalable and efficient structure with low complexity is proposed to determine the optimal day-ahead operation of the renewable power system in coordination with private IEHs within the privacy-preserving decision-making framework. In this regard, a decentralized two-stage robust-stochastic security-constrained unit commitment (SCUC) model is developed for the collaborative operation of networked IEHs and the renewable power system to facilitate the coordinated operation of RPSO and IEHOs as well as to preserve the operational privacy of these parties.

(2) A generalized Benders decomposition algorithm is employed to solve the proposed distributed robust-stochastic model, which is in line with the prevalent leader-followers (RPSO-IEHOs) relationships in the energy management of the integrated renewable energy system. In the formed decomposition-based program, RPSO and IEHOs seek common goals with respect to privacy provisions.

Table 1: Comparison of the contributions of related literature with the proposed structure.

References	Operation mode	Privacy	Coordinator	Resources	P2H storage	DRPs	Uncertainty modeling
[18]	Centralized	Sharing all data	Central supervisor	ECF + EES + RESs	✓	✓	IGDT
[19]	Centralized	Sharing all data	Central supervisor	ECF + EES + RESs	×	✓	Robust
[20]	Centralized	Sharing all data	Central supervisor	ECF + RESs	×	✓	Stochastic
[21]	Centralized	Sharing local data	Central supervisor	ECF + EES + RESs	×	×	Stochastic
[23]	Centralized	Sharing all data	Central supervisor	ECF + EES	×	×	Deterministic
[25]	Centralized	Sharing all data	Central supervisor	ECF + EES + RESs	×	✓	Stochastic
[26]	Decentralized	Sharing power trading amount	PSO	ECF + EES + RESs	×	×	Deterministic
[27]	Decentralized	Sharing power trading amount	PSO	ECF	×	×	Deterministic
[28]	Decentralized	Sharing power trading amount	PSO	ECF + EES + RESs	×	×	Robust
[29]	Decentralized	Sharing power trading amount	ESO	ECF + EES	×	×	Deterministic
[30]	Decentralized	Sharing power trading amount	ESO	ECF + EES + RESs	×	×	Robust
[31]	Decentralized	Sharing power trading amount	ESO	ECF + EES + RESs	×	×	Robust
Proposed model	Decentralized	Sharing power trading amount	RPSO	ECF + EES + RESs	✓	✓	Hybrid robust-stochastic

*Note: ECF-Energy conversion facilities; PSO-Power system operator; ESO-Energy system operator

(3) A hybrid robust-stochastic strategy is implemented to handle the enforced operational uncertainties associated with the renewable power output of WFs and PV parks and the energy demands of local industrial consumers, and also to create less conservative and more trustworthy approaches. In this regard, the robust optimization technique is employed to model uncertainties associated with WFs and PV parks output powers, and the two-stage stochastic approach is used to handle the uncertainties caused by the energy demands of local industrial consumers.

(4) In addition to the above points, the proposed joint optimization structure is extended based on the multi-energy DRP, EES, and P2H storage, as the flexibility options, to minimize the total operation cost, immunize the power system in confronting the challenges of high-power RESs, as well as enhance operational flexibilities of the renewable power system by increasing spinning reserve.

(5) In order to validate the feasibility of the optimization algorithm, insightful analysis and realistic experiments are carried out using the unique options of the DIgSILENT PowerFactory [32]. In this regard, the role of the IEHs in increasing renewable power system flexibility is analyzed when the planned outage is applied to one of the generation units.

The structure of this paper is organized as follows. Section 2 explains the proposed structure and presents the two-stage stochastic mathematical model for the optimal operation of the renewable power system in coordination with IEHs. The robust optimization method for handling the uncertainty of renewable power generation is presented in Section 3. In Section 4, the decentralized approach for the

collaborative operation of multiple networked IEHs and renewable power system is explained. The numerical simulation and results for evaluating the proposed structure are provided in Section 5. Finally, conclusions and future works are drawn in Section 6. The schematic overview of the whole paper is shown in Fig. 1.

Fig. 1: Conceptual diagram of the proposed strategy.

2. Formulation of the proposed structure

In this section, the proposed distributed optimization model is formulated to ensure the optimal collaborative operations of networked IEHs with the renewable power system in the presence of various flexibility tools. The proposed model is composed of several independent entities, which are operated by separate decision-makers. The main entity has to do with RPSO as well as the private owners of IEHs are considered as the rest of the independent entities. The graphical description of the proposed structure is shown in Fig. 2. As can be seen, an integrated renewable energy system comprises a set $\mathcal{H}$ of $H = |\mathcal{H}|$ IEHs, power transmission system interfaces, WFs, PV parks, and local industrial consumers. In the proposed structure, IEHs and local industrial consumers are managed by IEHOs, and the rest of the system, i.e., WFs, PV parks, and conventional thermal units, are managed by RPSO. Each IEH is equipped with combined heat and power (CHP) units, EES, and P2H storage. An IEH has two input ports, i.e., electricity and gas connectors, and two output ports, i.e., electricity and heat connectors. The input ports are related to the purchased energies from the renewable power system and natural gas network, and output ports are used for trading electricity and thermal energy with industrial consumers and the renewable power system. In other words, IEHOs interact with RPSO via bi-directional communications for creating an economical and secure operation using the constrained transmission system. On the contrary, IEHOs have one-way collaboration with natural gas (at input ports) and district heating (at output ports)

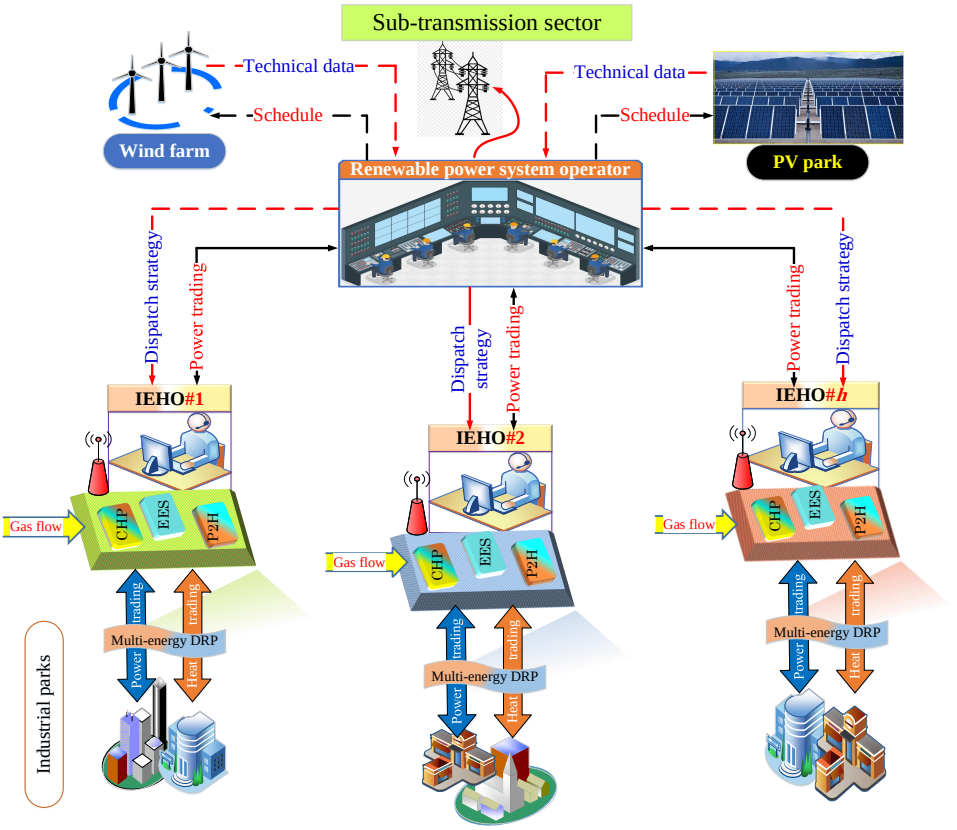

Fig. 2: Structure of decentralized operation for multiple networked IEHs.

networks. In the developed decentralized structure, the privacy of operation data is preserved since the RPSO will not need all operation data of IEHs. To preserve the private ownership of IEHOs, the conflicts of exchanging electrical power between RPSO and IEHOs are resolved by the Benders decomposition algorithm in an iterative procedure. In this regard, the integrated two-stage robust-stochastic optimization model is decomposed into a master problem and a set of sub-problems considering the uncertainties of wind and PV generation as well as electricity and heat demands in the industrial customers' side. The master problem is handled by RPSO to determine day-ahead robust SCUC, and sub-problems are solved independently by IEHOs for optimizing the operation of IEHs by relying on the two-stage stochastic programming. The details of the day-ahead robust-stochastic SCUC formulation for each decision-maker are described in the following sub-sections. At first, the two-stage stochastic SCUC problem is developed for the proposed privacy-preserving model, which will be updated in Section 3 to implement the hybrid robust-stochastic concept.

2.1. Decision-making of RPSO

The objective of RPSO's decision-making process is to minimize the total operation cost of supplying electrical loads outside of IEHs' services territories by thermal units and curtailing renewable power in optimal coordination with IEHOs over the entire day-ahead scheduling horizon. The objective function formed to model this process, which is given in (1), contains two stages. The first stage includes the costs

of start-up and shut-down of thermal units. This stage is independent of the stochastic process, therefore the start-up and shut-down costs are applied to all scenarios. The second stage of the objective function corresponds to the operation cost of thermal units and renewable power curtailment costs for WFs and PV parks. The second stage decision variables in the proposed two-stage stochastic programming model depend on the fluctuations in electricity and heat demands in the industrial customers' side, which are defined by different scenarios.

$$Min:$$

$$C^{RPS} = \sum_{t\in\mathcal{T}} \left[\sum_{g\in\mathcal{G}} (SUC_{g,t} + SDC_{g,t}) + \sum_{s\in\mathcal{S}} \sigma_s \cdot \left(\sum_{g\in\mathcal{G}} F_g(P_{g,t,s}) + \Pi_{re}(\sum_{w\in\mathcal{W}} PC_{w,t,s} + \sum_{p\in\mathcal{P}} PC_{p,t,s}) \right) \right] \tag{1}$$

2.1.1. Thermal units modeling

In this paper, the quadratic fuel cost function of thermal units is accurately approximated by a set of piecewise blocks to avoid complicating the optimization problem. The linearization process of the quadratic cost function using the least-squares criterion is illustrated in Fig. 3. The analytic representation of the linearization process is presented in (2)-(10) [33]. According to these equations, the fuel cost of thermal units can be defined by (10).

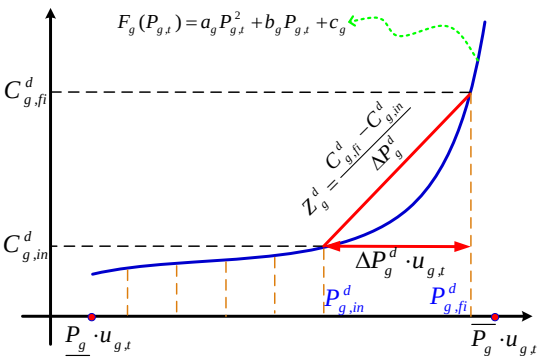

Fig. 3: Piecewise linear approximation of thermal units' quadratic cost function.

$$0 \le p^d_{g,t,s} \le \Delta P^d_g \cdot u_{g,t}, \qquad \forall g,t,s,d, \tag{2}$$

$$\Delta P^d_g = \frac{\overline{P_g} - \underline{P_g}}{\mathcal{D}}, \qquad \forall g,d, \tag{3}$$

$$P^d_{g,in} = (d-1)\cdot \Delta P^d_g + \underline{P_g}, \qquad \forall g,d, \tag{4}$$

$$P^d_{g,fi} = P^d_{g,in} + \Delta P^d_g, \qquad \forall g,d, \tag{5}$$

$$P_{g,t,s} = \underline{P_g} \cdot u_{g,t} + \sum_{d\in\mathcal{D}} p^d_{g,t,s}, \qquad \forall g,t,s, \tag{6}$$

$$C^d_{g,in} = a_g \cdot \left(P^d_{g,in}\right)^2 + b_g \cdot P^d_{g,in} + c_g, \qquad \forall g,d, \tag{7}$$

$$C^d_{g,fi} = a_g \cdot \left(P^d_{g,fi}\right)^2 + b_g \cdot P^d_{g,fi} + c_g, \quad \forall g, d, \tag{8}$$

$$Z^d_g = \frac{C^d_{g,fi} - C^d_{g,in}}{\Delta P^d_g}, \quad \forall g, d, \tag{9}$$

$$F_g(P_{g,t,s}) = a_g \cdot \underline{P_g}^2 + b_g \cdot \underline{P_g} + c_g \cdot u_{g,t} + \sum_{d \in \mathcal{D}} (Z^d_g \cdot p^d_{g,t,s}), \quad \forall g, t, s. \tag{10}$$

The technical constraints of thermal units are presented by (11)-(26) [34]. The thermal units ramp-rates constraints for continuous intervals are indicated by (11)-(18). The power produced by each thermal unit is limited by upper and lower bounds as expressed by (11). The upper bound of the accessible power output of thermal units is constrained by (12), i.e., shut-down ramp rate, and (13), i.e., ramp-up and start-up ramp rates. In addition, the lower bound of the accessible power output of thermal units is enforced by (15) and (16). Constraints (17) and (18) specify on/off states of all units.

$$P^{lo}_{g,t} \le P_{g,t,s} \le P^{up}_{g,t}, \quad \forall g, t, s, \tag{11}$$

$$P^{up}_{g,t} \le \bar{P}_g \cdot (u_{g,t} - \gamma_{g,t+1}) + SD_g \cdot \gamma_{g,t+1}, \quad \forall g, t, \tag{12}$$

$$P^{up}_{g,t} \le P_{g,t-1} + RU_g \cdot u_{g,t-1} + SU_g \cdot y_{g,t}, \quad \forall g, t, \tag{13}$$

$$P^{up}_{g,t} \ge 0, \quad \forall g, t, \tag{14}$$

$$P^{lo}_{g,t} \ge \underline{P_g} \cdot u_{g,t}, \quad \forall g, t, \tag{15}$$

$$P_{g,t-1} - P_{g,t} \le RD_g \cdot u_{g,t} + SD_g \cdot \gamma_{g,t}, \quad \forall g, t, \tag{16}$$

$$y_{g,t} - \gamma_{g,t} = u_{g,t} - u_{g,t-1}, \quad \forall g, t, \tag{17}$$

$$y_{g,t} + \gamma_{g,t} \le 1, \quad \forall g, t. \tag{18}$$

Inequities (19)-(26) express minimum up/down times limits of each thermal unit. Constraints (19)-(22) are applied to satisfy the minimum up time constraint in the initial, middle, and final periods of the scheduling horizon, respectively. Likewise, the minimum down time limits can be formulated as (23)-(26).

$$\sum_{t=1}^{\mu_g} (1 - u_{g,t}) = 0, \quad \forall g, \tag{19}$$

$$\mu_g = \min\left\{\mathcal{T}, (XG^{on}_g - UT^0_g) \cdot u_{g,0}\right\}, \quad \forall g, \tag{20}$$

$$\sum_{t=\nu}^{\nu+XG^{on}_g-1} u_{g,t} \ge XG^{on}_g \cdot y_{g,\nu}, \quad \forall g, \nu = [\mu_g + 1, ..., \mathcal{T} - XG^{on}_g + 1], \tag{21}$$

$$\sum_{t=\nu}^{\mathcal{T}} (u_{g,t} - y_{g,t}) \ge 0, \quad \forall g, \nu = [\mathcal{T} - XG^{on}_g + 2, ..., \mathcal{T}], \tag{22}$$

$$\sum_{t=1}^{\varsigma_g} u_{g,t} = 0, \quad \forall g, \tag{23}$$

$$\varsigma_g = \min\left\{\mathcal{T}, (XG_g^{off} - DT_g^0)\cdot(1-u_{g,0})\right\}, \quad \forall g, \tag{24}$$

$$\sum_{t=\nu}^{\nu+XG_g^{off}-1}(1-u_{g,t}) \geq XG_g^{off}\cdot\gamma_{g,\nu}, \quad \forall g, \nu = [\varsigma_g+1, ..., \mathcal{T}-XG_g^{off}+1], \tag{25}$$

$$\sum_{t=\nu}^{\mathcal{T}}(1-u_{g,t}-\gamma_{g,t}) \geq 0, \quad \forall g, \nu = [\mathcal{T}-XG_g^{off}+2, ..., \mathcal{T}]. \tag{26}$$

where μ_g and ς_g represent the numbers of initial periods that thermal unit g must be online and offline.

The start-up and shut-down costs are expressed as constant values as (27) and (28), respectively.

$$SUC_{g,t} \geq suc_g \cdot y_{g,t}; \quad SUC_{g,t} \geq 0, \quad \forall g, t, \tag{27}$$

$$SDC_{g,t} \geq sdc_g \cdot \gamma_{g,t}; \quad SDC_{g,t} \geq 0, \quad \forall g, t. \tag{28}$$

2.1.2. Renewable power system technical constraints

The technical and operational constraints (29)-(35) must be applied to the safe operation of the renewable power system [34]. Constraint (29) ensures the curtailment rate of each WF/PV park cannot exceed the forecast values. The linearized DC-power flow model is used to calculate the amount of power flows from bus i to bus j, which is presented in (30). The power flow in each line and voltage angle of each bus is restricted by its minimum and maximum limits, which are expressed by (31) and (32). It should be noted that the value of the voltage angle in the slack bus must be equal to zero. This critical constraint is expressed by (33). The electrical demands of the renewable power system should be met by the output power of the thermal units, WFs, PV parks, as well as the power exchanged with IEHs considering the power flow limits between the system buses. Hence, the power balance constraint at bus i can be described by (34). The amount of transferred power from the renewable power system to IEHs and vice versa should be limited by (35). Note that, $P_{h,t,s}$ is considered as a free variable. The positive amount shows the imported power from the renewable power system into the IEHs and the negative amount demonstrates the delivered power from IEHs into the renewable power system.

$$0 \leq PC_{x,t,s} \leq P_{x,t}^f, \quad \forall x \in \{w,p\}, t, s. \tag{29}$$

$$PF_{ij,t,s} = \frac{\delta_{i,t,s} - \delta_{j,t,s}}{x_{ij}}, \quad \forall i, j, t, s, \tag{30}$$

$$-\overline{PF_{ij}} \leq PF_{ij,t,s} \leq \overline{PF_{ij}}, \quad \forall i, j, t, s, \tag{31}$$

$$-\pi \leq \delta_{i,t,s} \leq +\pi, \quad \forall i, t, s, \tag{32}$$

$$\delta_{slack,t,s} = 0, \quad \forall t, s, \tag{33}$$

$$\begin{aligned}&\sum_{g\in\mathcal{G}} KN_{i,g}\cdot P_{g,t,s} + \sum_{w\in\mathcal{W}} KN_{i,w}\cdot(P_{w,t}^f - PC_{w,t,s}) + \sum_{p\in\mathcal{P}} KN_{i,p}\cdot(P_{p,t}^f - PC_{p,t,s}) - \\ &\sum_{h\in\mathcal{H}} KN_{i,h}\cdot P_{h,t,s} - \sum_{m\in\mathcal{M}} KN_{i,m}\cdot PD_{m,t} = \sum_{j\in\mathcal{I}} KN_{i,j}\cdot PF_{ij,t,s}, \quad \forall i, t, s,\end{aligned} \tag{34}$$

$$\underline{P_h} \leq P_{h,t,s} \leq \overline{P}_h, \quad \forall h, t, s. \tag{35}$$

2.2. Decision-making of individual IEHs

Each IEH ($\forall h$) possesses EES, CHP unit, and P2H storage as the energy conversion facilities, for supplying local electricity and heat demands in industrial parks while interacting with RPSO. In the proposed decentralized approach, the energy hub model can be easily developed to include other energy conversion facilities. In the decision-making process of each IEH, the aim is to minimize the total operation cost of each IEH over the entire day-ahead scheduling horizon, considering the uncertainty of local industrial consumers' demands. The objective function of private IEHs is formulated in (36) as follows:

$$\begin{aligned} &Min: \\ &C_h^{IEH} = \sum_{s\in\mathcal{S}} \sigma_s [\sum_{k\in\mathcal{K}} C_{k,s}^{CHP} + \sum_{q\in\mathcal{Q}} C_{q,s}^{P2H} + \sum_{e\in\mathcal{E}} C_{e,s}^{ES} + \sum_{\substack{(l,n)\in \\ (\mathcal{L},\mathcal{N})}} C_{l,n,s}^{MDR}], \quad \forall h. \end{aligned} \tag{36}$$

The first term of (36), i.e., $C_{k,s}^{CHP}$, indicates the fuel and maintenance costs of CHP units, which can be calculated by (37) [35]. The second term, i.e., $C_{q,s}^{P2H}$, refers to the maintenance cost of P2H storages, which can be defined by (38). The EES degradation cost, i.e., $C_{e,s}^{ES}$, due to frequent charge and discharge, is considered in the third term. The accumulated degradation cost of EESs in IEHs are characterized by (39) [29]. Eventually, the final term, i.e., $C_{l,n,s}^{MDR}$, of (36) represents the multi-energy DRP compensation cost, where the incentive compensation costs paid to the industrial customers to perform the multi-energy DRP can be defined as (40) [36]. These cost functions are determined by the optimal scheduling of private IEHs in the optimal coordinated operation with the renewable power system. It should be noted that $H_{q,t,s}$ and $P_{e,t,s}$ are considered as free variables in (38) and (39).

$$C_{k,s}^{CHP} = \sum_{t\in\mathcal{T}} (\frac{\lambda_g}{\eta_k \cdot HV} \cdot P_{k,t,s}) + (\rho_k \cdot P_{k,t,s}), \quad \forall k, s, \tag{37}$$

$$C_{q,s}^{P2H} = \sum_{t\in\mathcal{T}} \rho_q \cdot H_{q,t,s}, \quad \forall q, s, \tag{38}$$

$$C_{e,s}^{ES} = \sum_{t\in\mathcal{T}} \rho_e \cdot P_{e,t,s}, \quad \forall e, s, \tag{39}$$

$$C_{l,n,s}^{MDR} = \sum_{t\in\mathcal{T}} \left[\Big(IE \times (\Delta P_{l,t,s}^{up} + \Delta P_{l,t,s}^{dw}) \Big) + \Big(IH \times (\Delta H_{n,t,s}^{up} + \Delta H_{n,t,s}^{dw}) \Big) \right], \quad \forall l, n, s. \tag{40}$$

The operational constraints governing IEHs are described below.

2.2.1. CHP units constraints

The heat and electric power produced by CHP units have mutual dependence, which is determined by the special feasible operation region (FOR) for each unit. The feasible region model associated with the considered CHP units in this article is shown in Fig. 4. The operational boundary (ABCD) of CHP units can be formulated by linear constraints, as given in (41)-(43) [37]. In these constraints, M is a large number, e.g., 1000. Moreover, constraints (44) and (45) ensure that the power and heat production of CHP units are at acceptable levels.

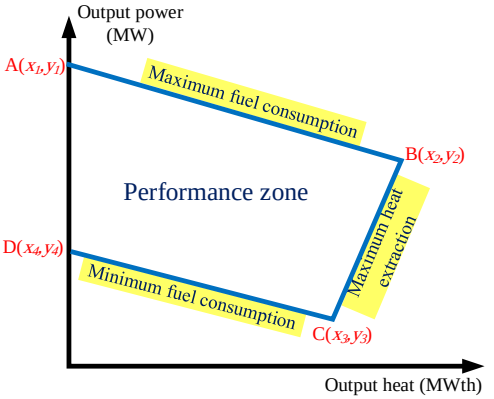

Fig. 4: FOR model for CHP units.

$$P_{k,t,s} - P_{k,A} - \frac{P_{k,A} - P_{k,B}}{H_{k,A} - H_{k,B}} \cdot (H_{k,t,s} - H_{k,A}) \leq 0, \qquad \forall k, t, s, \tag{41}$$

$$P_{k,t,s} - P_{k,B} - \frac{P_{k,B} - P_{k,C}}{H_{k,B} - H_{k,C}} \cdot (H_{k,t,s} - H_{k,B}) \geq -(1 - u_{k,t,s}) \cdot M, \qquad \forall k, t, s, \tag{42}$$

$$P_{k,t,s} - P_{k,C} - \frac{P_{k,C} - P_{k,D}}{H_{k,C} - H_{k,D}} \cdot (H_{k,t,s} - H_{k,C}) \geq -(1 - u_{k,t,s}) \cdot M, \qquad \forall k, t, s, \tag{43}$$

$$\underline{P_k} \leq P_{k,t,s} \leq \overline{P_k}, \qquad \forall k, t, s, \tag{44}$$

$$0 \leq H_{k,t,s} \leq \overline{H_k}, \qquad \forall k, t, s. \tag{45}$$

2.2.2. P2H storages constraints

The operational constraints related to P2H storages are defined as (46)-(51). The dynamic energy balance of the P2H storage in each hour is expressed by (46). The capacity limit of the P2H storage is given by (47). The initial ($t = 0$) and final ($t = \mathcal{T}$) state of charge of the P2H storage is limited to (48). The allowable ranges of charging/discharging thermal energy in this storage are limited by (49). The generated thermal energy by the P2H storage can be delivered to the industrial customers or district heating networks, as stated in (50). Here, constraint (51) demonstrates the allowable limit for input power from the renewable power system into the P2H storage.

$$A_{q,t,s} = (1 - \eta_q) \cdot A_{q,t-1,s} + H_{q,t,s} - \beta_{loss} \cdot SU_{q,t,s} + \beta_{gain} \cdot SD_{q,t,s}, \qquad \forall q, t, s, \tag{46}$$

$$\underline{A_q} \leq A_{q,t,s} \leq \overline{A_q}, \qquad \forall q, t, s, \tag{47}$$

$$A_{q,0,s} = A_{q,\mathcal{T},s}, \qquad \forall q, s, \tag{48}$$

$$0 \leq H_{q,t,s} \leq \overline{H_q}, \qquad \forall q, t, s, \tag{49}$$

$$H^{dir}_{q,t,s} = COP_q \cdot P_{q,t,s}, \qquad \forall q, t, s, \tag{50}$$

$$0 \leq P_{q,t,s} \leq \overline{P_q}, \qquad \forall q, t, s. \tag{51}$$

2.2.3. EES system constraints

The operation of each EES is defined by the following relationships. Based on (52), the electrical energy level of each EES in a scheduling interval is calculated. The capacity level of each EES should be restricted in its minimum and maximum limits, which is modeled by (53). According to (54), the state of charge of each EES must be equal to $A_{e,0,s}$ at the end of the scheduling period. The charge/discharge limitation of each EES is imposed by (55).

$$A_{e,t,s} = A_{e,t-1,s} + \eta_e \cdot P_{e,t,s}, \quad \forall e, t, s, \tag{52}$$

$$\underline{A_e} \leq A_{e,t,s} \leq \overline{A_e}, \quad \forall e, t, s, \tag{53}$$

$$A_{e,0,s} = A_{e,\tau,s}, \quad \forall e, s, \tag{54}$$

$$0 \leq P_{e,t,s} \leq \overline{P_e}, \quad \forall e, t, s. \tag{55}$$

2.2.4. Multi-energy DRP constraints

DRP is one of the most flexible tools for the management of IEHs behavior to interact effectively with the renewable power system by exploiting the economic opportunities available in the industrial customers' side. In this paper, multi-energy DRP is performed to minimize the total operation cost of the integrated renewable energy system, reduce renewable power curtailments, and enhance the flexibility of the renewable power system by creating optimal coordination between RPSO and each IEHO in an iterative manner. DRPs are divided into two categories: the price-based DRP and the incentive-based DRP. In this study, multi-energy DRP is considered based on the incentive-based manner, which is performed using direct load control (DLC) program. Hence, the incentive compensation costs are paid to the participating customers in the form of the DLC program. Based on (56) and (57), the DLC program is performed on the electrical and heat demands with respect to the percentage of participation of each consumer in the multi-energy DRP. After the implementation of multi-energy DRP, the final electrical and heat profiles are determined using (58) and (59) [36].

$$\begin{cases} \Delta P^{up}_{l,t,s} \leq \alpha_l \times PD^{ini}_{l,t,s}, & \forall l, t, s, \\ \Delta P^{dw}_{l,t,s} \leq \alpha_l \times PD^{ini}_{l,t,s}, & \forall l, t, s, \end{cases} \tag{56}$$

$$\begin{cases} \Delta H^{up}_{n,t,s} \leq \alpha_n \times HD^{ini}_{n,t,s}, & \forall n, t, s, \\ \Delta H^{dw}_{n,t,s} \leq \alpha_n \times HD^{ini}_{n,t,s}, & \forall n, t, s, \end{cases} \tag{57}$$

$$PD^{dr}_{l,t,s} = \Delta P^{up}_{l,t,s} - \Delta P^{dw}_{l,t,s} + PD^{ini}_{l,t,s}, \quad \forall l, t, s, \tag{58}$$

$$HD^{dr}_{n,t,s} = \Delta H^{up}_{n,t,s} - \Delta H^{dw}_{n,t,s} + HD^{ini}_{n,t,s}, \quad \forall n, t, s. \tag{59}$$

2.2.5. IEHs' energy balancing

Each IEHO manages the energy balance in each IEH by considering localized energy generation, energy curtailments, as well as power imported/exported from/to the renewable power system. Constraints (60) and (61) are used to make the energy balance between energy consumed by local demands, i.e., $PD^{dr}_{l,t,s}$ and $HD^{dr}_{n,t,s}$, and generated/traded energy in each IEH. It should be noted that the modified energy demands after implementing multi-energy DRP are used rather than the initial energy demands in the supply-demand constraints.

$$P_{h,t,s} + \sum_{e\in E} KN_{h,e}\cdot P_{e,t,s} + \sum_{k\in\mathcal{K}} KN_{h,k}\cdot P_{k,t,s} - \sum_{q\in\mathcal{Q}} KN_{h,q}\cdot P_{q,t,s} - \sum_{l\in\mathcal{L}} KN_{h,l}\cdot PD^{dr}_{l,t,s} = 0, \quad \forall h,t,s, \tag{60}$$

$$\sum_{k\in\mathcal{K}} KN_{h,k}\cdot H_{k,t,s} + \sum_{q\in\mathcal{Q}} KN_{h,q}\cdot (H_{q,t,s} + H^{dir}_{q,t,s}) - \sum_{n\in\mathcal{N}} KN_{h,n}\cdot HD^{dr}_{n,t,s} = 0, \quad \forall h,t,s. \tag{61}$$

3. Hybrid robust-stochastic model

In the above-described model, the uncertainty of renewable generation was neglected and the output power of WFs and PV parks was perfectly forecasted. Since the uncertainty of RESs is more vital than the energy demands, the RPSO prefers to apply a risk-based method to handle the uncertainty associated with renewable powers, while the IEHOs try to manage the fluctuations of electrical and heat demands of local industrial consumers using stochastic programming based on a Monte-Carlo (MC) simulation. Compared to stochastic programming, which requires the probability distribution function (PDF) or fuzzy membership set of uncertain parameters, the robust approach describes uncertain parameters by descriptive statistics. Therefore, in such models, complex calculations resulting from scenario counting are avoided. In the proposed privacy-preserving decision-making structure, the mathematical definition of the distributed robust-stochastic approach to realize the worst case is as follows.

After adopting the budget of uncertainty, the uncertainty set of WFs and PV parks is described by (62)-(64) [38]. The degree of uncertainty of RESs in period t can be controlled by variable $\beta_{x,t,s}$. The value of $\beta_{x,t,s} = 0$ demonstrates that there is no uncertainty in renewable power production in period t, while $\beta_{x,t,s} = 1$ demonstrates that the maximum renewable power uncertainty occurs in period t. The robustness level of the solution can be controlled by the budget of uncertainty, i.e., Γ_t. The budget of the uncertainty parameter can change from 0 to 1 in each scheduling interval. The greater value of Γ_t, e.g., 1, means that RPSO has selected a highly conservative state in period t. In contrast, a lower value of Γ_t means that the uncertain parameter is almost neglected in period t.

$$P_{x,t} \in \left[P^f_{x,t} - \beta_{x,t,s}\cdot\tilde{P}_{x,t}, P^f_{x,t} + \beta_{x,t,s}\cdot\tilde{P}_{x,t}\right], \quad \forall x\in\{w,p\},t,s, \tag{62}$$

$$0 \le \beta_{x,t,s} \le 1, \quad \forall x\in\{w,p\},t,s, \tag{63}$$

$$\sum_{w\in\mathcal{W}} \beta_{w,t,s} + \sum_{p\in\mathcal{P}} \beta_{p,t,s} \le \Gamma_t, \quad \forall t,s. \tag{64}$$

Based on the uncertainty model of the RESs presented in (62)-(64), the renewable power curtailment constraint, which was shown in (29), and energy balance constraint, which was shown in (34), can be

converted to (65) and (66), respectively.

$$0 \leq PC_{x,t,s} \leq P^{f}_{x,t} + \max_{\beta_{x,t,s}}[\beta_{x,t,s} \cdot \tilde{P}_{x,t}], \qquad \forall x \in \{w,p\}, t, s, \tag{65}$$

$$\begin{aligned} &\max_{\beta_{x,t,s}}[\sum_{x\in\mathcal{X}} KN_{i,x} \cdot (P^{f}_{x,t} - \beta_{x,t,s} \cdot \tilde{P}_{x,t})] = \sum_{x\in\mathcal{X}} KN_{i,x} \cdot PC_{x,t,s} + \sum_{m\in\mathcal{M}} KN_{i,m} \cdot PD_{m,t} + \\ &\sum_{j\in\mathcal{I}} KN_{i,j} \cdot PF_{ij,t,s} - \sum_{g\in\mathcal{G}} KN_{i,g} \cdot P_{g,t,s} - \sum_{h\in\mathcal{H}} KN_{i,h} \cdot P_{h,t,s}, \qquad \forall x \in \{w,p\}, i, t, s. \end{aligned} \tag{66}$$

Subject to: (63) and (64)

By applying the robust approach, the RPSO faces a bilevel min-max optimization problem. The duality theory can be used to handle the bilevel optimization problem. Hence, the min-max optimization problem is converted into a min-min program using the duality theory. According to the introduced mechanism in [39], constraint (66) can be converted to (67)-(69) using the duality theory.

$$\begin{aligned} &\min_{r_{x,t,s},\varepsilon_{t,s}} [\sum_{x\in\mathcal{X}} KN_{i,x} \cdot (P^{f}_{x,t} - r_{x,t,s}) - (\varepsilon_{t,s} \cdot \Gamma_t)] = \sum_{x\in\mathcal{X}} KN_{i,x} \cdot PC_{x,t,s} + \sum_{m\in\mathcal{M}} KN_{i,m} \cdot PD_{m,t} + \\ &\sum_{j\in\mathcal{I}} KN_{i,j} \cdot PF_{ij,t,s} + \sum_{h\in\mathcal{H}} KN_{i,h} \cdot P_{h,t,s} - \sum_{g\in\mathcal{G}} KN_{i,g} \cdot P_{g,t,s}, \qquad \forall x \in \{w,p\}, i, t, s, \end{aligned} \tag{67}$$

$$\min_{r_{x,t,s},\varepsilon_{t,s}} [r_{x,t,s} + \varepsilon_{t,s}] \geq \tilde{P}_{x,t}, \qquad \forall x \in \{w,p\}, t, s, \tag{68}$$

$$r_{x,t,s}, \varepsilon_{t,s} \geq 0, \qquad \forall x \in \{w,p\}, t, s. \tag{69}$$

where $r_{x,t,s}$ and $\varepsilon_{t,s}$ are the dual variables of the initial problem. The constraint (65) can also be transformed into (70) based on the duality theory.

$$0 \leq PC_{x,t,s} \leq P^{f}_{x,t} + \min_{r_{x,t,s},\varepsilon_{t,s}} [r_{x,t,s} + \varepsilon_{t,s} \cdot \Gamma_t], \qquad \forall x \in \{w,p\}, t, s. \tag{70}$$

After performing this mathematical process, the distributed robust-stochastic SCUC model can be formulated as mixed-integer linear programming (MILP) problem, which can be solved using commercial optimization packages. The summary of the proposed model is as follows.

- **Objective function of the leader:** RPSO aims to minimize the total operating cost by (1).
- Constraints of the leader problem:
  1. Applying thermal unit constraints based on (2)-(28).
  2. Applying renewable power curtailments constraints based on (70).
  3. Satisfying technical limitations based on (30)-(33), (35), and (67)-(69).
- **Objective function of the followers:** Each IEHO aims to minimize their own operating costs by (36)- (40).
- Constraints of the follower problems:

1. Applying CHP units constraints based on (41)-(45).
2. Applying P2H storages constraints based on (46)-(51).
3. Applying EES systems constraints based on (52)-(55).
4. Performing multi-energy DRP based on (56)-(59).
5. Satisfying energy balance limitations based on (60) and (61).

4. Decentral solution methodology

The proposed distributed robust-stochastic SCUC problem is in an MILP format that guarantees the global optimal solution. However, the operating problem of the renewable power system and IEHs are interdependent through (67), which due to this constraint, it is not possible to solve the optimization problems separately. Based on (67), the RPSO and IEHOs are coupled with the hourly scheduling and exchange of electrical power at IEHs' nodes. To address this issue, the standard Benders decomposition algorithm is applied to solve the proposed collaborative operation model in a decentralized manner while preserving the privacy of RPSO and IEHOs. Benders decomposition algorithm is one of the most efficient decomposition techniques, which is used in power systems. The details of the implementation of the Benders decomposition algorithm are given in [40].

The Benders decomposition can be utilized to exploit a separable framework for the two-stage robust-stochastic SCUC problem, where this problem is decomposed into an optimization problem as a master problem for RPSO and several optimal operation problems at the level of IEHOs as sub-problems, which will be solved separately.

(I) **Master problem (MP)**: RPSO is responsible for ensuring the operational security of the renewable power system and tries to minimize the total operation cost, including operation cost of thermal units and compensation cost of renewable power curtailments according to the optimal trade policy of power with IEHs. The general structure of the master problem at iteration t_b is formulated as (71).

$$\begin{aligned} &Min: \quad \hat{O}_{t_b}^{Total}, \\ &\hat{O}_{t_b}^{Total} = C^{RPS} + \sum_{h \in \mathcal{H}} O_h^{app}, \\ &s.t. \quad \text{Operational constraints of the leader problem,} \\ &\qquad \text{Feasibility cutting plane,} \\ &\qquad \text{Optimality cutting plane.} \end{aligned} \tag{71}$$

where O_h^{app} is a non-negative continuous variable that represents the operation cost of the IEH h as approximated by the RPSO. At each iteration, RPSO minimizes the total operation cost, i.e., $\hat{O}_{t_b}^{Total}$, as an effective lower bound (LB) of the optimal robust-stochastic SCUC model by considering all available Benders cuts constraints ($LB = \hat{O}_{t_b}^{Total}$).

(II) **Sub-problem of the h^{th} IEH**: After solving the master problem at each iteration, the optimal power trade schedule in the form of a tentative solution is passed to sub-problems that can be handled

in parallel by individual IEHs. The IEHOs determine the optimal dispatch of IEHs in two phases. In the first phase, IEHOs check whether the power exchange schedule obtained from the master problem is practically feasible by considering operational and technical constraints in each IEH operation. The feasibility check sub-problem for the h^{th} IEH at iteration t_b is stated as:

$$\begin{aligned} Min: \quad & \hat{F}^{IEH}_{t_b,h,t,s} = \xi^{P1}_{h,t,s} + \xi^{P2}_{h,t,s}, \\ s.t. \quad & \text{Operational constraints of followers problems,} \\ & P_{h,t,s} + \xi^{P1}_{h,t,s} = \hat{P}_{t_b,h,t,s} + \xi^{P2}_{h,t,s}; \qquad (\Lambda^{P}_{t_b,h,t,s}), \\ & \xi^{P1}_{h,t,s}, \xi^{P2}_{h,t,s} \geq 0. \end{aligned} \tag{72}$$

where $\hat{P}_{t_b,h,t,s}$ is related to the power exchange amounts, which is obtained from the master problem. Moreover, $\xi^{P1}_{h,t,s}$ and $\xi^{P2}_{h,t,s}$ are non-negative slack variables, and $\Lambda^{P}_{t_b,h,t,s}$ is the dual variable associated with the first constraint of the problem (72). For a non-zero optimal objective value ($\hat{F}^{IEH}_{t_b,h,t,s} \neq 0$), the determined power trade schedule via the master problem is infeasible. Hence, inequality (73) as the feasibility cut should be created and provided back to the master problem.

$$\hat{F}^{IEH}_{t_b,h,t,s} + \Lambda^{P}_{t_b,h,t,s} \cdot \left(P_{h,t,s} - \hat{P}_{t_b,h,t,s} \right) \leq 0. \tag{73}$$

But if the optimal objective value $\hat{F}^{IEH}_{t_b,h,t,s}$ equals to zero, the determined power trade schedule will be feasible. In this case, the optimal values of all slack variables will be equal to zero. Upon completion of the feasibility check phase, the IEHOs will solve the optimality sub-problems in the second phase as presented in (74).

$$\begin{aligned} Min: \quad & \hat{O}^{IEH}_{t_b,h}, \\ & \hat{O}^{IEH}_{t_b,h} = \sum_{s \in \mathcal{S}} \sigma_s \cdot [\sum_{k \in \mathcal{K}} C^{CHP}_{k,s} + \sum_{e \in \mathcal{E}} C^{ES}_{e,s} + \sum_{q \in \mathcal{Q}} C^{P2H}_{q,s} + \sum_{\substack{(l,n) \in \\ (\mathcal{L},\mathcal{N})}} C^{MDR}_{l,n,s}], \\ s.t. \quad & \text{Operational constraints of followers problems,} \\ & P_{h,t,s} = \hat{P}_{t_b,h,t,s} \qquad (\tau^{P}_{t_b,h,t,s}). \end{aligned} \tag{74}$$

where $\hat{O}^{IEH}_{t_b,h}$ signifies the minimized operation cost for the h^{th} IEH under the determined power trade schedule, and $\tau^{P}_{t_b,h,t,s}$ is the dual variable associated with the constraint of the problem (74). After that, an effective upper bound (UB) of the optimal two-stage robust-stochastic SCUC model can be calculated by (75).

$$UB = \hat{O}^{Total}_{t_b} + \sum_{h \in \mathcal{H}} (\hat{O}^{IEH}_{t_b,h} - O^{app}_{h}). \tag{75}$$

In each iteration, the convergence criterion of the Benders decomposition algorithm must be checked to decide whether it is necessary to perform the next iteration. A generally used convergence criterion is

stated below:

$$|UB - LB| \leq \varepsilon. \tag{76}$$

where ε is a pre-defined value that indicates the convergence threshold. But if the convergence criterion is not met, the optimality cut should be constructed according to (77), and then added to the master problem. The flowchart of the proposed problem-solving process is shown in Fig. 5.

$$\hat{O}^{IEH}_{t_b,h} + \tau^{P}_{t_b,h,t,s} \cdot \left(P_{h,t,s} - \hat{P}_{t_b,h,t,s}\right) \leq O^{app}_{h}. \tag{77}$$

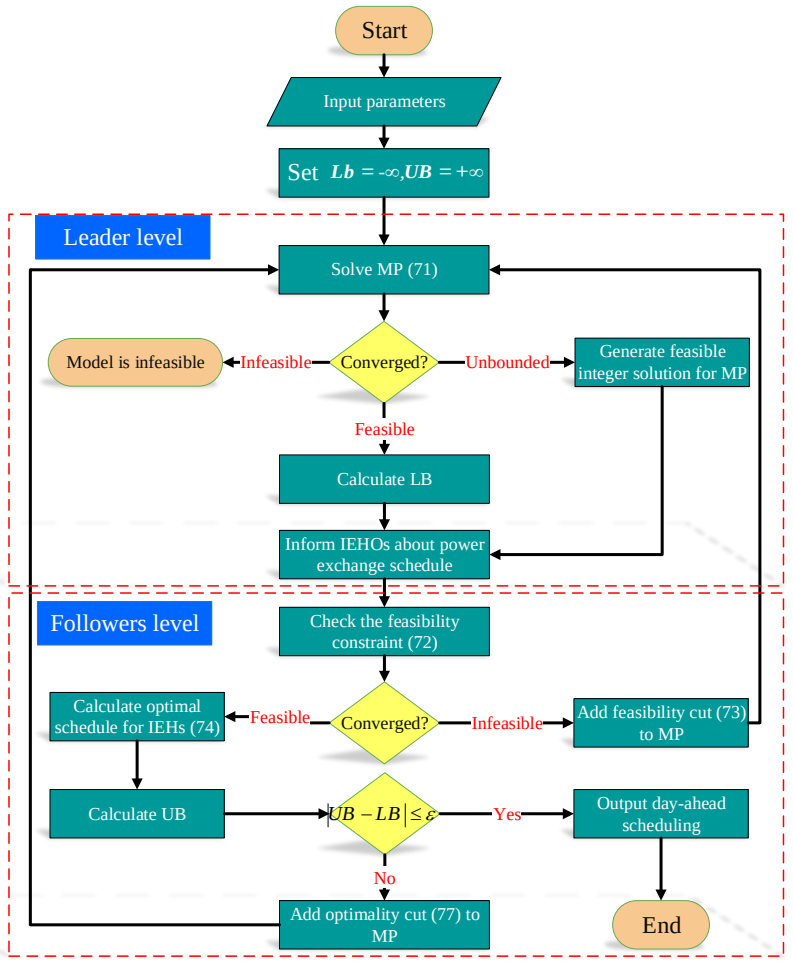

Fig. 5: Flowchart of the proposed algorithm.

5. Case study and numerical results

In this section, the developed collaborative decision-making structure is applied to the modified IEEE 30-bus test system to validate the feasibility and efficiency of the proposed decentral optimization program. The scheduling horizon is one day ($\mathcal{T} = 24$) with one-hour time slots. The numerical case studies are implemented in the environment of GAMS software on a personal computer with an Intel CoreTM i7-4500 CPU and 6-GB RAM. The proposed MILP problem is solved by commercial solver CPLEX in which the

relative gap and the solution time limits are adjusted to 0.1% and 10000 s. Moreover, the convergence tolerance of the Benders decomposition algorithm is set at 0.05%.

5.1. Simulation setup

The topology of the modified test system is shown in Fig. 6. This test system is composed of two integrated areas. The first area is related to the renewable power system, which includes 30 buses, six conventional thermal units, 2 WFs, 2 PV parks, and 21 electrical loads. It should be noted that these electrical loads represent the transmission substations in the test system. Bus 1 represents the slack bus, with a voltage phase angle of zero. All technical specifications associated with the 30-bus test system are provided in [41]. It should be noted that the capacity of transmission lines and technical parameters of thermal units were adjusted according to the peak load. The second area covers the two industrial parks that are equipped with IEHs. IEHs are committed to providing the electrical and heat demands of local industrial consumers located in industrial parks. Two IEHs are respectively located at buses 21 and 30, which are indicated by IEH1 and IEH2. Each IEH consists of a CHP unit, an EES system, and a P2H storage. Thus, in the whole integrated renewable energy system, there are two CHP units, two EES systems, and two P2H storages.

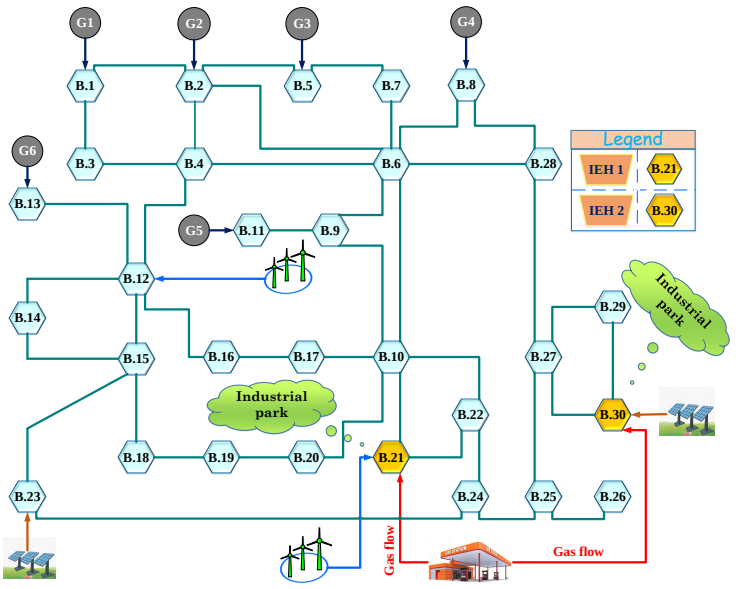

Fig. 6: Schematic of the proposed test system.

The predicted values related to each WF and PV park productions, as well as the hourly forecasted energy demands of all entities, are shown in Figs. 7 and 8. The rated capacity of WFs, PV parks installed on buses 12, 21, 23, and 30 are equal to 275, 325, 185, and 335 MW, respectively. It should be mentioned that candidate buses for the installation of RESs were selected in accordance with the results of the planning study carried out in [42]. In addition, all RESs produce active power at unity power factor. The share of each bus from the hourly electrical demand is acquired from PowerFactory's library. The heat loads connected to the buses 21 and 30 have 40% and 60% share of the total heat demand, respectively. The characteristics of energy conversion facilities installed in IEHs are adopted from [43] and scaled to

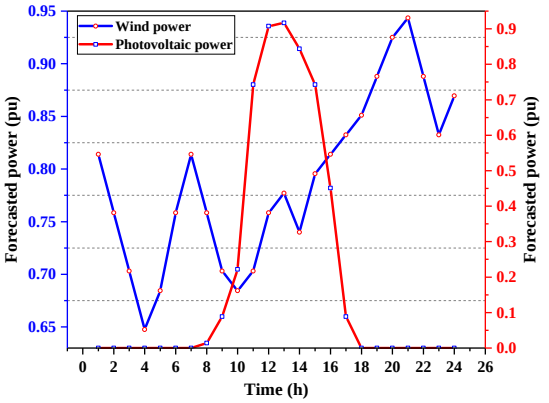

Fig. 7: Forecasted output power of each WF and PV park.

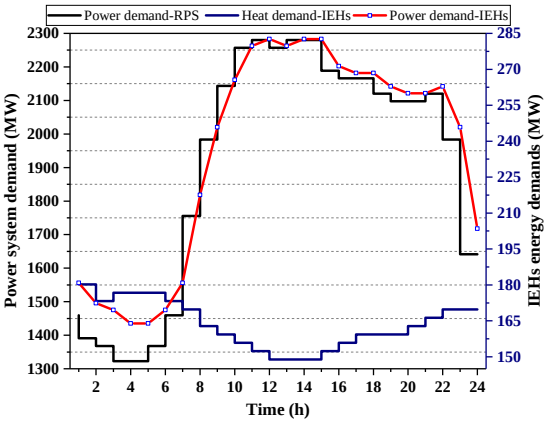

Fig. 8: Forecasted electricity and heat demands.

achieve 180 MW of thermal energy. The essential technical characteristics are given in Table 2.

The penalty cost of renewable power curtailment, i.e., Π_{re}, is set to 20 \$/MW that is higher than the highest marginal cost of available thermal units, and the natural gas price, i.e., λ_g, is assumed to be 15 \$/MWh [43]. The maintenance costs of CHP units, i.e., ρ_k, and P2H storages, i.e., ρ_q, are considered 43.2 \$/MW and 10 \$/MW, respectively [44]. Also, the EES degradation cost, i.e., ρ_e, is 10 \$/MW [29]. The incentive values for implementing multi-energy DRP are set to 20 \$/MWh and 10 \$/MWh for the electrical and heat loads, respectively. Furthermore, the coefficients α_l and α_n are assumed to be 15% and 10%, respectively.

Six case studies are considered to investigate the impact of the proposed structure on improving the

Table 2: Specifications of the available equipment in IEHs.

Parameter	Amount	Parameter	Amount
η_k, η_q, η_e	0.35, 0.05, 0.9	$\underline{A_q}, \overline{A_q}$ (MWh)	0, 60
$\underline{P_k}, \overline{P_k}$ (MW)	35, 130	$\overline{P_e}$ (MW)	20
$\underline{H_k}, \overline{H_k}$ (MW)	0, 110	$\underline{A_e}, \overline{A_e}$ (MWh)	0, 60
$\overline{P_q}$ (MW)	40	$\beta_{loss}, \beta_{gain}$	0.3, 0.6
$\overline{H_q}$ (MW)	20	COP_q	1.5

performance of the integrated renewable energy system. These include:

- *Base case*: In the base case, high-renewable power system is operated without the deployment of IEHs;
- *Case 1*: The optimal collaborative operation of the high-renewable power system and IEHs is analyzed in a decentralized manner. In this case, IEHs are equipped with only CHP units and various uncertain parameters are not considered;
- *Case 2*: The EES system is plugged into existing IEHs, and then the effects of electrical storage on case 1 are investigated;
- *Case 3*: Case 2 is developed by considering the role of P2H storage in achieving the desired goals;
- *Case 4*: The benefits of implementing multi-energy DRP on improving the techno-economic performance of the integrated renewable energy system are evaluated according to the IEHs formed in case 3. In this case, the uncertainties of renewable power production and energy demands are also ignored.
- *Case 5*: The proposed robust-stochastic SCUC model is applied to manage the uncertainties of the renewable power production and energy demands of the local industrial consumers with respect to privacy provisions. In this case, multi-energy DRP and all energy conversion facilities are considered.

5.2. Comparative results with/without various tools

To perform the collaborative operation scheme in terms of power trades, RPSO and IEHOs optimize the scheduling of local energy resources by satisfying several operational/technical constraints in the renewable power system and IEHs. Figs. 9 and 10 show the total operation cost of the renewable power system and IEHs at each iteration of the Benders process for each case study. As can be seen, it takes 4, 4, 5, and 5 iterations to reach optimal results in cases 1 to 4, respectively. After proceeding with the iterations, RPSO coordinates the scheduled power exchange with IEHOs at each hour, according to the governing targets in each entity.

The hourly traded power between IEH1/IEH2 and the renewable power system for each case study are shown in Figs. 11 and 12, respectively. The negative values for traded power indicate that IEHs are willing to deliver the surplus power to the renewable power system. As can be seen in these figures, regarding the capacity in each industrial park, IEH1 has more power demand from the renewable power system than IEH2 during the scheduling horizon. Meanwhile, IEH2 exhibits a higher tendency to transfer power to the renewable power system, specifically during the final intervals of the scheduling horizon. In both industrial areas, the highest traded power between IEHs and the renewable power system is related to case 3, where P2H storages are exploited as an efficient energy conversion facility.

Tables 3 and 4 present the total electrical and heat demands supplied by different resources for each case study. As it is evident from Table 3, the IEHs act as a viable option to increase the hosting capacity of RESs in meeting the electricity demand of the integrated renewable energy system. On the other hand, in case 2, the power generated by thermal units during the scheduling horizon decreased by about 3,200.604 MW compared to the base case (without the deployment of IEHs). Therefore, the amount of spinning

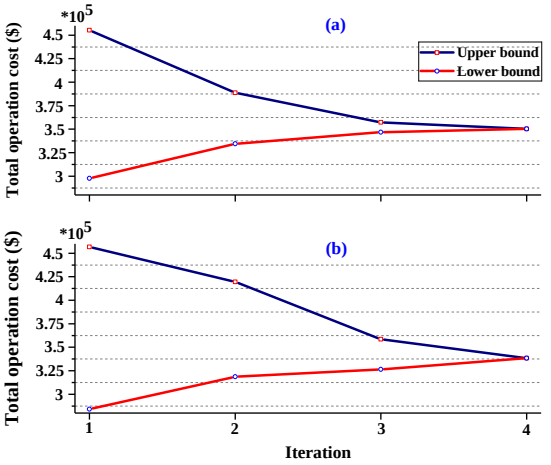

Fig. 9: Iteration process of Benders decomposition for (a) case 1 and (b) case 2.

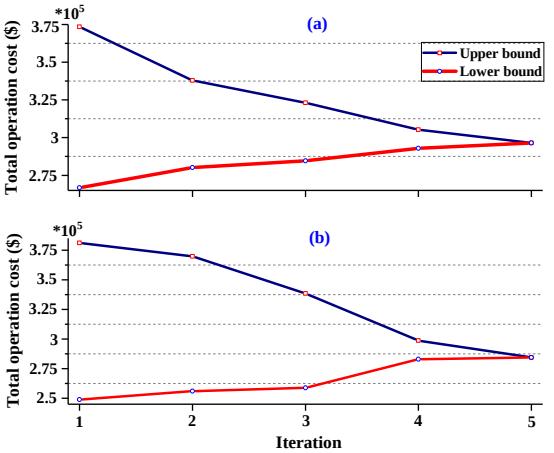

Fig. 10: Iteration process of Benders decomposition for (a) case 3 and (b) case 4.

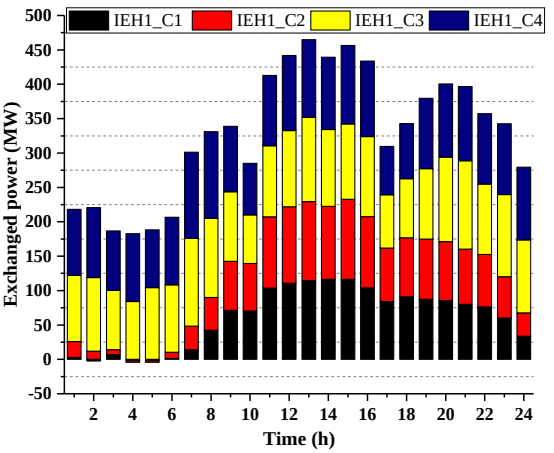

Fig. 11: Hourly traded power between IEH1 and renewable power system for each case study at bus 21.

reserve provided by thermal units can increase by up to 9.67% by adopting the optimal coordinated strategy between the renewable power system and IEHs. In addition, case 4 demonstrates the capability of the proposed multi-energy DRP to enhance the reliability of the integrated renewable energy system by

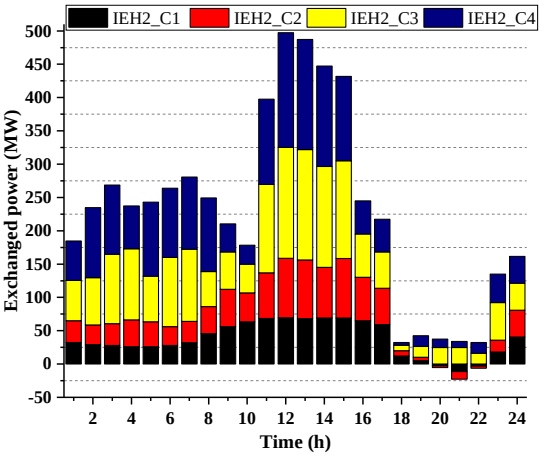

Fig. 12: Hourly traded power between IEH2 and renewable power system for each case study at bus 30.

Table 3: Optimal mix of various sources to procure total electrical demand for each case study.

	Base case	Case 1	Case 2	Case 3	Case 4
Production of thermal units (MW)	33,081.634	29,894.483	29,881.03	31,409.356	31,288.961
Production of RESs (MW)	13,555.256	13,463.434	13,583.318	13,940.739	13,945.96
Production of CHP units (MW)	-	3,278.973	3,202.407	1,941.63	1,516.058
Production of EESs in discharging mode (MW)	-	-	134.392	141.85	129.09
Power delivered to EESs in charging mode (MW)	-	-	-164.257	-173.372	-157.777
Power delivered to P2H storages (MW)	-	-	-	-623.314	-646.593
Curtailed load in multi-energy DRP (MW)	-	-	-	-	561.191
Total electrical demand (MW)			**46,636.89**		

Table 4: Optimal mix of various sources to procure total heat demand for each case study.

	Case 1	Case 2	Case 3	Case 4
Production of CHP units (MW)	3,938.609	3,938.609	3,079.862	2,810.623
Production of P2H storages in direct mode (MW)	-	-	866.155	933.863
Production of P2H storages in discharging mode (MW)	-	-	61.407	32.551
Heat delivered to P2H storages in charging mode (MW)	-	-	-68.816	-36.025
Curtailed load in multi-energy DRP (MW)	-	-	-	197.597
Total heat demand (MW)		**3,938.609**		

curtailing electrical demand (about 561 MW) using the DLC program. The distribution of the required demand among different sources, which are supported by different energy carriers, increases the flexibility and resilience of the renewable power system against potential risks associated with non-dispatchable power sources, natural disasters, and cyber attacks. From the heating point of view, CHP units act as the main supplier to cover the heat demand of industrial parks, which is due to its high production capacity.

The total amount of renewable power curtailment in each WF and PV park for each case study are also presented in Figs. 13 and 14. The results demonstrate that the proposed privacy-preserving structure is able to dramatically reduce renewable power curtailment with optimal collaborative expansion scheduling. In accordance with case 2, by adding EESs to IEHs under the title of backup power stations, it is found

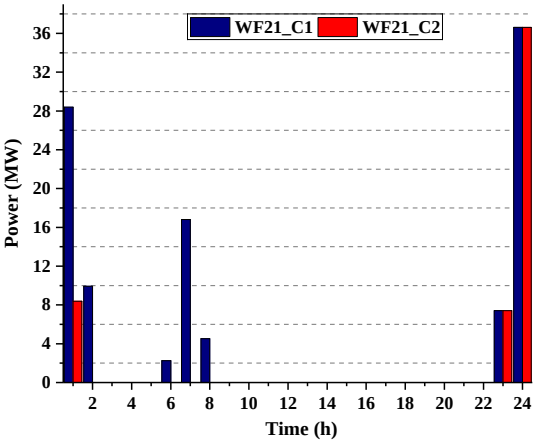

Fig. 13: Wind power curtailment for each case study.

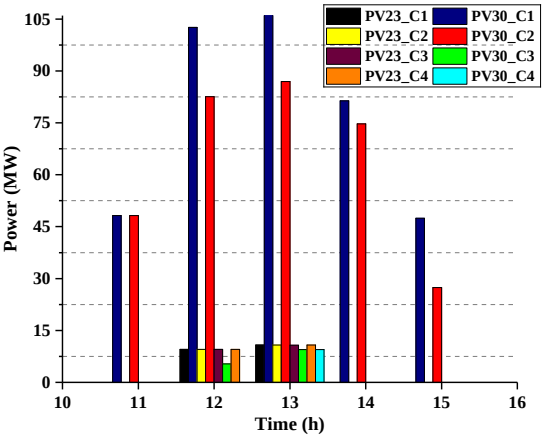

Fig. 14: Solar power curtailment for each case study.

that the amount of curtailed renewable power reduces by 23.44% when compared to case 1. In case 3, the amount of curtailed renewable power significantly decreases in comparison with cases 1 and 2 by incorporating the unique capabilities of P2H storages in the collaborative scheme to determine the power trading schedule. In addition, with the simultaneous use of P2H storages and multi-energy DRP in the collaborative scheduling approach among RPSO and IEHOs, the values of curtailed wind and solar power had reached zero and 29.85 MW, respectively. These simulation results clearly reveal that the promoted IEHs in optimal coordination with the renewable power system had an effective role in reducing renewable power curtailment.

In case 4, the effects of multi-energy DRP in coordination with EESs and P2H storages are evaluated on the performance of IEHs to achieve the desired targets. It is assumed that the multi-energy DRP is implemented only on the local industrial energy demands, which are located at buses 21 and 30. Figs. 15 and 16 show the consequence of implementing multi-energy DRP on the electrical and heat demands of the industrial consumers connected to IEHs. According to these figures, the total electrical and heat demands of the industrial consumers reduce by up to 9.94% and 5.017%, respectively, which is one of the reasons for improving the performance of the integrated renewable energy system from the technical

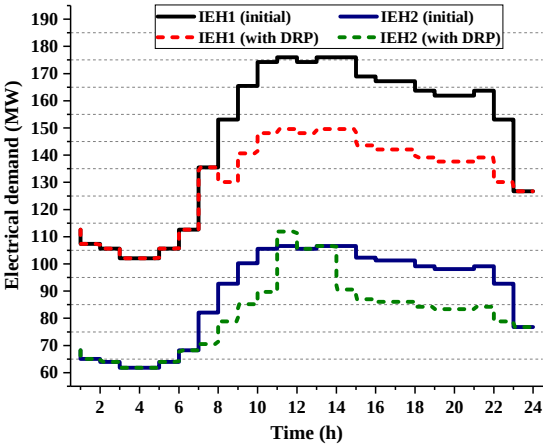

Fig. 15: The effect of multi-energy DRP on the local electrical demand of IEHs.

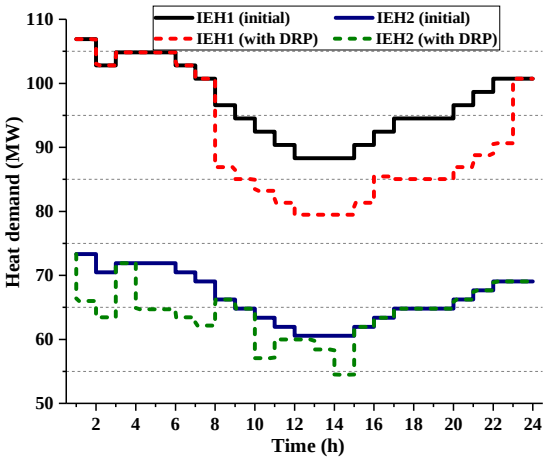

Fig. 16: The effect of multi-energy DRP on the local heat demand of IEHs.

perspective.

Table 5 presents a comprehensive economic comparison of different scheduling scenarios. As it is shown, the total operation cost of the renewable power system can be significantly reduced by deploying IEHs in industrial parks according to a decentralized collaborative operation. In accordance with case 1, with establishing IEHs along with the renewable power system under the title of sustainable energy producers, it is found that the amount of total operation cost of renewable power system decreases by 11.41% when compared to the base case. Moreover, the operation cost of the renewable power system decreases by up to 16.33% in case 2, 11.6% in case 3, and 14.19% in case 4 compared to the base case by adding EESs and P2H storage to each IEH as well as utilizing multi-energy DRP in the framework of IEHs. On the other hand, the total operation cost of IEHs reduces from \$141,660 (case 1) to \$88,332.899 (case 3) by using EESs and P2H storages. Finally, by examining the renewable power curtailment cost, which is reduced from \$8,411.139 to \$597.043 by implementing the proposed privacy-preserving decision-making structure, the impact of applying multi-energy DRP in the objective function is clearly revealed. It can be seen that the amount of renewable power curtailment cost in case 1, when IEHs are only equipped with CHP units, is higher than other case studies. These results prove the necessity of using flexibility tools in the form of

IEHs.

Table 5: Cost allocation for existing entities for each case study.

	Base case	Case 1	Case 2	Case 3	Case 4
Operation cost of thermal units ($)	226,996	198,300	189,110	207,400	201,400
Cost of renewable power curtailment ($)	8,411.139	10,253.354	7,849.882	701.456	597.043
Total operation cost of renewable power system ($)	235,407.139	208,553.354	196,959.882	208,101.456	201,997.043
Renewable power system operation cost decrement (%)	-	11.41	16.33	11.60	14.19
Operation cost of energy conversion facilities ($)	-	141,660	141,330	88,332.899	69,048.178
Incentive compensation costs of multi-energy DRP ($)	-	-	-	-	13,412.37
Total operation cost of IEHs ($)	-	141,660	141,330	88,332.899	82,460.548

5.3. Sensitivity analysis

In this sub-section, three sensitivity analyses are conducted to assess the importance of the introduced flexibility options on renewable power curtailment as well as the total operation cost of IEHs. These analyses are very useful for IEHOs and RPSO to harness existing opportunities in the energy markets. All assumptions are the same as those of case 4. Fig. 17 shows the sensitivity of the amount of renewable power curtailment and operation cost of IEHs to variations of the multi-energy DRP participation rate, i.e., α_l and α_n. The participation rates of electrical and heat demands for implementing multi-energy DRP changed from $(\alpha_{l,n} - 8)\%$ to $(\alpha_{l,n} + 10)\%$ applying nine equal steps. As can be seen from Fig. 17, the total operation cost of IEHs decreases almost nonlinearly. On the other hand, there are almost no changes in the renewable power curtailment up to values close to $(\alpha_l + 4)\%$ and $(\alpha_n + 4)\%$. But, the renewable power curtailment dramatically increases with increasing the participation rates of electrical and heat demands to more than $(\alpha_l + 4)\%$ and $(\alpha_n + 4)\%$. These results indicate that it is necessary to perform a trade-off between different targets for the ideal utilization of the multi-energy DRP. In Fig. 18, the sensitivity of the renewable power curtailment and operation cost of IEHs is analyzed by assigning different values of incentive compensation costs. In this analysis, the incentive values for implementing multi-energy DRP, i.e., (IE, IH) are incremented/decremented by (2 $/MWh, 1 $/MWh) steps regarding the base values of (20 $/MWh, 10 $/MWh). As it can be derived, the rate of renewable power curtailment and the operation cost of IEHs significantly increase with increasing the amounts of (IE, IH).

The effect of the coefficient of performance (COP) of P2H storage on the amount of renewable power curtailment and the total operation cost of IEHs is shown in Fig. 19. As it is obvious, the increase in COP of P2H units dramatically reduces both renewable power curtailment and operation cost of IEHs. Therefore, the efficiency of the proposed strategy can be strengthened with the use of high-efficiency P2H storage.

5.4. Monitoring the loading of thermal units

In order to validate the feasibility of the optimization algorithm as well as to evaluate the rate of the spinning reserve of thermal units, the thermal units' loading level is monitored using DIgSILENT

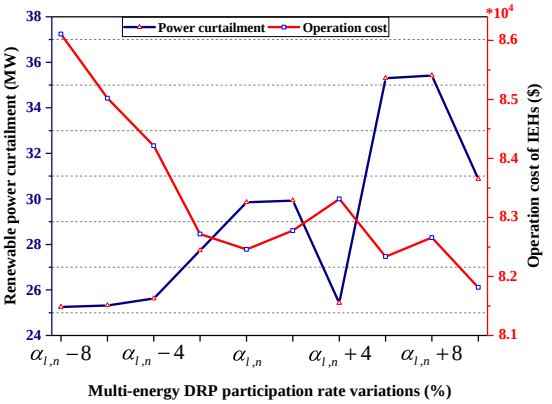

Fig. 17: Sensitivity of renewable power curtailment and operation cost of IEHs to α_l and α_n.

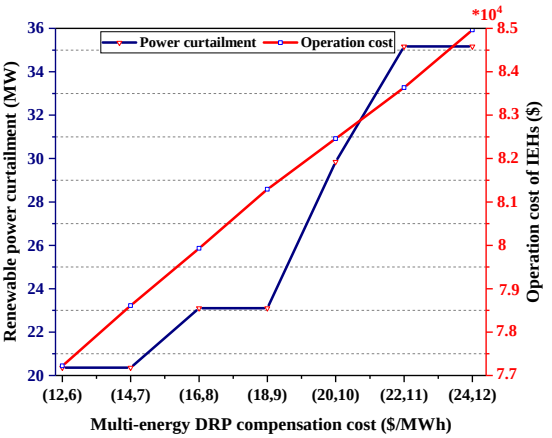

Fig. 18: Sensitivity of renewable power curtailment and operation cost of IEHs to *IE* and *IH*.

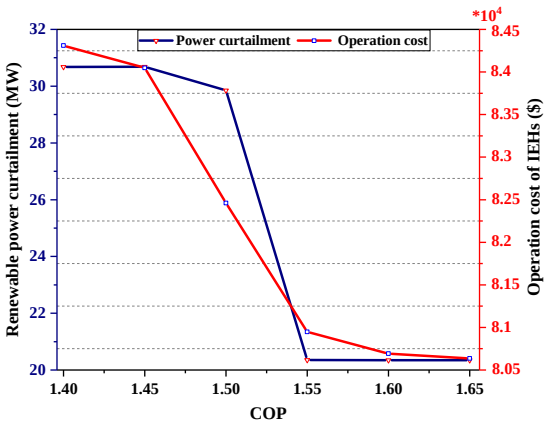

Fig. 19: Sensitivity of renewable power curtailment and operation cost of IEHs to the coefficient of P2H performance.

PowerFactory software in different operating conditions after implementing the optimization process. In the first stage, the original test system is modeled in the software according to the considered assumptions. Then, the efficient Quasi-Dynamic Simulation tool is applied to analyze the IEEE 30-bus test system. Fig. 20(a) shows the thermal units' loading range for the base case. As it is evident, G1 has the highest loading range, i.e., 68.2%. To evaluate the efficiency of the proposed strategy in abnormal conditions of

the renewable power system, it is assumed that a planned outage occurred in G3 from t=11 to t=15 to carry out emergency repairs. Fig. 20(b) shows the status of thermal units when G3 was not under load. As can be seen, the most critical situation of the thermal units' loading level with 105.6% is related to G2, which is increased by 45.9% compared to the normal condition in the base case. Nevertheless, the loading level of G2 is improved with the optimal operation of the renewable power system in coordination with private IEHs within the privacy-preserving framework. As can be seen in Fig. 20(c), the loading level of G2 in case 4 (with the optimal deployment of IEHs along with DRP) is decreased to 82.6% under the defined planned outage. Reducing the thermal units' loading level indicates the increase in the spinning reserve of the renewable power system. The obtained results demonstrate the extraordinary technical effect of using IEHs in coordination with the renewable power system.

5.5. Impacts of uncertain parameters

In case 5, the impacts of uncertain parameters, i.e., renewable power production and electrical and heat demands of local industrial consumers, on the results of the collaborative operation are investigated using the adjusted hybrid robust-stochastic model to more clearly technical and economic analysis. The energy demand prediction error follows a normal distribution function with a deviation of 10% and a mean of zero. To this end, one-hundred scenarios are generated by MC simulation, which is reduced to ten scenarios by the GAMS/SCENRED tool [45]. To handle the uncertainty associated with renewable power production, the value of uncertainty budget, i.e., Γ_t, in the robust model is increased by steps 0.02 from 0.02 to 0.2. To carry out the desired simulations, three different ranges for the maximum deviation between the forecasted and actual values, i.e., $\tilde{P}_{x,t}$, are considered. The variation in the operation costs of the renewable power system and IEHs for different Γ_t when $\tilde{P}_{x,t}$ changes from 10% to 30% are shown in Figs. 21 and 22. As can be seen in Fig. 21, with increasing the amounts of Γ_t and $\tilde{P}_{x,t}$, the operation cost of the renewable power system increases. The reason is that higher uncertainty budgets force RPSO

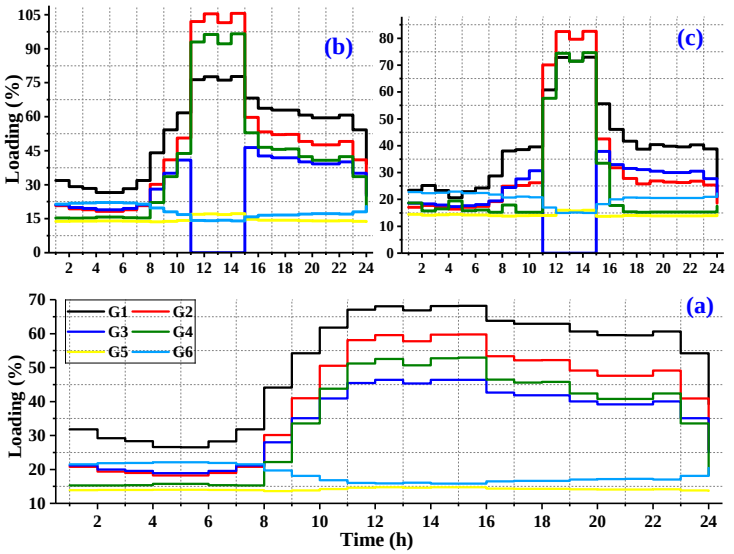

Fig. 20: Thermal units' loading range for: (a) base case without planned outage; (b) base case with the planned outage in G3; (c) case 4 with the planned outage in G3.

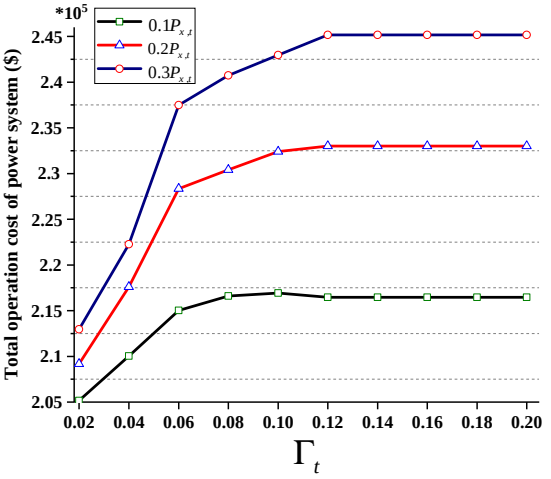

Fig. 21: Impact of Γ_t and $\tilde{P}_{x,t}$ on total operation cost of renewable power system.

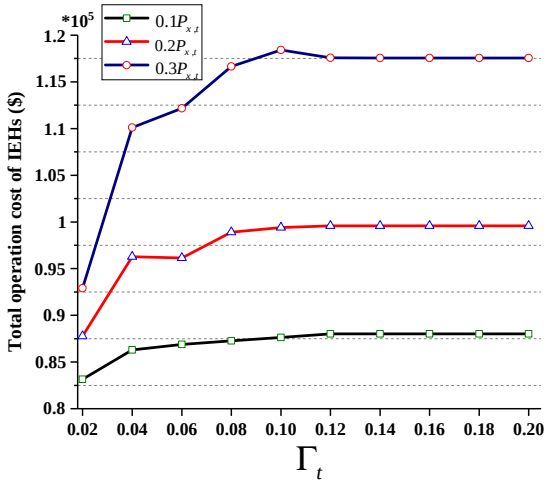

Fig. 22: Impact of Γ_t and $\tilde{P}_{x,t}$ on total operation cost of IEHs.

to provide the required power from expensive units instead of the RESs. Similarly, according to Fig. 22, with increasing the robust approach parameters, the operation cost of IEHs also grows. As it is anticipated, the expected operation costs of IEHs and renewable power system have increased under the uncertainty environment compared to the deterministic condition due to reduced participation of high-power RESs. As can be seen from these figures, the total operation costs of IEHs and renewable power systems stabilize for Γ_t higher than 0.12. Traded power between IEH1/IEH2 and the renewable power system for $0.1P_{x,t}$ is shown in Fig. 23. As clearly visible, the total traded power between IEH1/IEH2 and renewable power system decreases from 3627.38 MW, when $\Gamma_t = 0.02$, to 3623.58 MW, when $\Gamma_t = 0.2$, during the scheduling horizon. This is due to the fact that by reducing the actual power generated by RESs compared to the forecasted value, i.e., $\Gamma_t = 0$, the traded power between IEHs and the renewable power system also decreases.

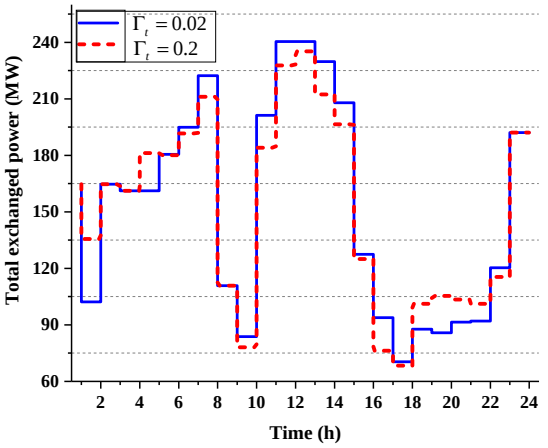

Fig. 23: The effect of variations of the uncertainty budgets on the total exchanged power.

6. Conclusions and future work

This paper presented a decentralized two-stage robust-stochastic model to achieve the optimal collaborative operation of private industrial energy hubs with the renewable power system in a privacy-preserving manner. In the presented collaboration structure, a renewable power system operator interacted with industrial energy hubs in leader-followers fashion to perform the security-constrained unit commitment problem, while the Benders decomposition algorithm was exploited to resolve the conflicts of private entities. The main goals of the developed privacy-preserving decision-making structure were to decrease the rate of renewable power curtailment as well as to minimize the operation costs of each private entity by relying on establishing a sustainable power trading schedule between industrial energy hub operators and renewable power system operator. The proposed model considered uncertainties in renewable energy sources power and energy demands of local industrial consumers, where combined heat and power unit, electrical energy storage, power-to-heat storage, and multi-energy demand response program served as the backup energy supply units in the framework of industrial energy hubs. The obtained numerical results in the IEEE 30-bus test system confirmed the effectiveness of the proposed decentral solution in creating an economical and secure operation between industrial energy hubs and renewable power systems. The key findings from the simulation studies could be drawn as:

(1) Deploying the industrial energy hubs in the industrial parks had an undeniable role in minimizing the total operation cost of the renewable power system. In the worst case, industrial energy hubs were able to reduce the operation cost of the renewable power system by 11.41% compared to the initial state of the renewable power system.

(2) Utilizing the flexibility options such as power-to-heat storage and multi-energy demand response program had a significant effect on the rate of renewable power curtailment. The renewable power curtailment was decreased by up to 92.9% in the presence of flexibility tools.

(3) Using the two-stage robust-stochastic approach enabled the renewable power system operator and industrial energy hub operators to adjust the robustness level of the optimization process, as well as to cover the uncertainty of renewable power and energy demands in real-time decisions.

(4) DIgSILENT PowerFactory validated the practical feasibility of implementing the proposed optimization strategy under normal and abnormal conditions. By using the capabilities of this software, the thermal units' loading level was monitored when an event occurred in a part of the power system.

In future work, we will focus on the transactive energy mechanism between multiple networked industrial energy hubs to enhance the flexibility and resiliency of the integrated renewable energy system.

Acknowledgment

Amjad Anvari-Moghaddam and Behnam Mohammadi acknowledge the support of the "HeatReFlex-Green and Flexible Heating/Cooling" project (www.heatreflex.et.aau.dk) funded by Danida Fellowship Centre and the Ministry of Foreign Affairs of Denmark under the grant no. 18-M06-AAU.

References

[1] M. Peker, A. S. Kocaman, B. Y. Kara, Benefits of transmission switching and energy storage in power systems with high renewable energy penetration, Applied Energy 228 (2018) 1182 – 1197.

[2] M. Zare Oskouei, A. Sadeghi Yazdankhah, Scenario-based stochastic optimal operation of wind, photovoltaic, pump-storage hybrid system in frequency- based pricing, Energy Conversion and Management 105 (2015) 1105 – 1114.

[3] W. Wang, B. Sun, H. Li, Q. Sun, R. Wennersten, An improved min-max power dispatching method for integration of variable renewable energy, Applied Energy 276 (2020) 115430.

[4] M. Z. Oskouei, B. Mohammadi-Ivatloo, M. Abapour, R. Razzaghi, Two-stage stochastic model for optimal scheduling of reconfigurable active distribution networks with renewable energy, in: 2019 9th International Conference on Power and Energy Systems (ICPES), 2019, pp. 1–5.

[5] G. S. Seck, V. Krakowski, E. Assoumou, N. Maïzi, V. Mazauric, Embedding power system's reliability within a long-term energy system optimization model: Linking high renewable energy integration and future grid stability for france by 2050, Applied Energy 257 (2020) 114037.

[6] Electric power annual 2014, u.s. energy information administration (EIA), [online]. available at: http://www.eia.gov/electricity/annual/pdf/epa.pdf (2016).

[7] M. R. Akhtari, M. Baneshi, Techno-economic assessment and optimization of a hybrid renewable co-supply of electricity, heat and hydrogen system to enhance performance by recovering excess electricity for a large energy consumer, Energy Conversion and Management 188 (2019) 131 – 141.

[8] O. Abedinia, M. Zareinejad, M. H. Doranehgard, G. Fathi, N. Ghadimi, Optimal offering and bidding strategies of renewable energy based large consumer using a novel hybrid robust-stochastic approach, Journal of Cleaner Production 215 (2019) 878 – 889.

[9] S. Yazdani, M. Deymi-Dashtebayaz, E. Salimipour, Comprehensive comparison on the ecological performance and environmental sustainability of three energy storage systems employed for a wind farm by using an emergy analysis, Energy Conversion and Management 191 (2019) 1 – 11.

[10] X. Chen, C. Kang, M. O'Malley, Q. Xia, J. Bai, C. L. *et al.*, Increasing the flexibility of combined heat and power for wind power integration in china: Modeling and implications, IEEE Transactions on Power Systems 30 (4) (2015) 1848–1857.

[11] S. Rahmani, N. Amjady, Optimal operation strategy for multi-carrier energy systems including various energy converters by multi-objective information gap decision theory and enhanced directed search domain method, Energy Conversion and Management 198 (2019) 111804.

[12] T. Liu, D. Zhang, S. Wang, T. Wu, Standardized modelling and economic optimization of multi-carrier energy systems considering energy storage and demand response, Energy Conversion and Management 182 (2019) 126 – 142.

[13] Z. Jiang, Q. Ai, R. Hao, Integrated demand response mechanism for industrial energy system based on multi-energy interaction, IEEE Access 7 (2019) 66336–66346.

[14] S. O. Sobhani, S. Sheykhha, R. Madlener, An integrated two-level demand-side management game applied to smart energy hubs with storage, Energy 206 (2020) 118017.

[15] C. Dang, J. Zhang, C. Kwong, L. Li, Demand side load management for big industrial energy users under blockchain-based peer-to-peer electricity market, IEEE Transactions on Smart Grid 10 (6) (2019) 6426–6435.

[16] M. J. Shabani, S. M. Moghaddas-Tafreshi, Fully-decentralized coordination for simultaneous hydrogen, power, and heat interaction in a multi-carrier-energy system considering private ownership, Electric Power Systems Research 180 (2020) 106099.

[17] H. Gao, S. Xu, Y. Liu, L. Wang, Y. Xiang, J. Liu, Decentralized optimal operation model for cooperative microgrids considering renewable energy uncertainties, Applied Energy 262 (2020) 114579.

[18] M. Zare Oskouei, B. Mohammadi-Ivatloo, M. Abapour, M. Shafiee, A. Anvari-Moghaddam, Techno-economic and environmental assessment of the coordinated operation of regional grid-connected energy hubs considering high penetration of wind power, Journal of Cleaner Production 280 (2021) 124275.

[19] X. Lu, Z. Liu, L. Ma, L. Wang, K. Zhou, S. Yang, A robust optimization approach for coordinated operation of multiple energy hubs, Energy 197 (2020) 117171.

[20] M. H. Shams, M. Shahabi, M. Kia, A. Heidari, M. Lotfi, M. S. khah *et al.*, Optimal operation of electrical and thermal resources in microgrids with energy hubs considering uncertainties, Energy 187 (2019) 115949.

[21] A. A. Eladl, M. I. El-Afifi, M. A. Saeed, M. M. El-Saadawi, Optimal operation of energy hubs integrated with renewable energy sources and storage devices considering CO_2 emissions, International Journal of Electrical Power & Energy Systems 117 (2020) 105719.

[22] Z. Li, Y. Xu, Temporally-coordinated optimal operation of a multi-energy microgrid under diverse uncertainties, Applied Energy 240 (2019) 719 – 729.

[23] T. Liu, D. Zhang, T. Wu, Standardised modelling and optimisation of a system of interconnected energy hubs considering multiple energies—electricity, gas, heating, and cooling, Energy Conversion and Management 205 (2020) 112410.

[24] Z. Li, Y. Xu, Optimal coordinated energy dispatch of a multi-energy microgrid in grid-connected and islanded modes, Applied Energy 210 (2018) 974 – 986.

[25] A. Bostan, M. S. Nazar, M. Shafie-khah, J. P. Catalão, Optimal scheduling of distribution systems considering multiple downward energy hubs and demand response programs, Energy 190 (2020) 116349.

[26] X. Wang, Y. Liu, C. Liu, J. Liu, Coordinating energy management for multiple energy hubs: From a transaction perspective, International Journal of Electrical Power & Energy Systems 121 (2020) 106060.

[27] S. Bahrami, F. Aminifar, Exploiting the potential of energy hubs in power systems regulation services, IEEE Transactions on Smart Grid 10 (5) (2019) 5600–5608.

[28] N. Nikmehr, Distributed robust operational optimization of networked microgrids embedded interconnected energy hubs, Energy 199 (2020) 117440.

[29] Y. Li, Z. Li, F. Wen, M. Shahidehpour, Privacy-preserving optimal dispatch for an integrated power distribution and natural gas system in networked energy hubs, IEEE Transactions on Sustainable Energy 10 (4) (2019) 2028–2038.

[30] Y. Zhou, M. Shahidehpour, Z. Wei, Z. Li, G. Sun, S. Chen, Distributionally robust co-optimization of energy and reserve for combined distribution networks of power and district heating, IEEE Transactions on Power Systems 35 (3) (2020) 2388–2398.

[31] Y. Zhou, M. Shahidehpour, Z. Wei, Z. Li, G. Sun, S. Chen, Distributionally robust unit commitment in coordinated electricity and district heating networks, IEEE Transactions on Power Systems 35 (3) (2020) 2155–2166.

[32] M. Zare Oskouei, B. Mohammadi-Ivatloo, Integration of renewable energy sources into the power grid through powerfactory, 1st Edition, Springer International Publishing, 2020.

[33] M. Carrion, J. M. Arroyo, A computationally efficient mixed-integer linear formulation for the thermal unit commitment problem, IEEE Transactions on Power Systems 21 (3) (2006) 1371–1378.

[34] M. Yan, N. Zhang, X. Ai, M. Shahidehpour, C. Kang, J. Wen, Robust two-stage regional-district scheduling of multi-carrier energy systems with a large penetration of wind power, IEEE Transactions on Sustainable Energy 10 (3) (2019) 1227–1239.

[35] F. Teymoori Hamzehkolaei, N. Amjady, A techno-economic assessment for replacement of conventional fossil fuel based technologies in animal farms with biogas fueled chp units, Renewable Energy 118 (2018) 602 – 614.

[36] M. Zare Oskouei, A. Sadeghi Yazdankhah, The role of coordinated load shifting and frequency-based pricing strategies in maximizing hybrid system profit, Energy 135 (2017) 370 – 381.

[37] M. Alipour, K. Zare, B. Mohammadi-Ivatloo, Short-term scheduling of combined heat and power generation units in the presence of demand response programs, Energy 71 (2014) 289 – 301.

[38] M. Mohiti, H. Monsef, H. Lesani, A decentralized robust model for coordinated operation of smart distribution network and electric vehicle aggregators, International Journal of Electrical Power & Energy Systems 104 (2019) 853 – 867.

[39] D. Bertsimas, M. Sim, Robust discrete optimization and network flows, Mathematical Programming 98 (2003) 49 – 71.

[40] Z. Yuan, M. R. Hesamzadeh, Hierarchical coordination of tso-dso economic dispatch considering large-scale integration of distributed energy resources, Applied Energy 195 (2017) 600 – 615.

[41] H. Mohsenian-Rad, Coordinated price-maker operation of large energy storage units in nodal energy markets, IEEE Transactions on Power Systems 31 (1) (2016) 786–797.

[42] K. Tian, W. Sun, D. Han, C. Yang, Coordinated planning with predetermined renewable energy generation targets using extended two-stage robust optimization, IEEE Access 8 (2020) 2395–2407.

[43] M. A. Mirzaei, M. Z. Oskouei, B. Mohammadi-Ivatloo, A. Loni, K. Zare, M. M. *et al.*, Integrated energy hub system based on power-to-gas and compressed air energy storage technologies in the presence of multiple shiftable loads, IET Generation, Transmission & Distribution 14 (2020) 2510–2519.

[44] M. Jadidbonab, B. Mohammadi-Ivatloo, M. Marzband, P. Siano, Short-term self-scheduling of virtual energy hub plant within thermal energy market, IEEE Transactions on Industrial Electronics (2020) 1–1.

[45] Gams/scenred user guide, 2009. [online]. available at: http://www.gams.com/.